

2-Methoxyestradiol and Analogs as Novel Antiproliferative Agents: Analysis of Three-Dimensional Quantitative Structure-Activity Relationships for DNA Synthesis Inhibition and Estrogen Receptor Binding

RICHARD A. HUGHES, TRUDI HARRIS, EMILE ALTMANN, DAVID MCALLISTER, ROSS VLAHOS, ALAN ROBERTSON, MARK CUSHMAN, ZHIQIANG WANG, AND ALASTAIR G. STEWART

Departments of Pharmacology (R.A.H., T.H., E.A., R.V., A.G.S.) and Chemistry (D.M.), University of Melbourne, Melbourne, Victoria, Australia; Department of Medicinal Chemistry and Molecular Pharmacology, Purdue University, West Lafayette, Indiana (M.C., Z.W.); and Baker Medical Research Institute, Prahran, Victoria, Australia (A.R.)

Received December 13, 2001; accepted February 11, 2002

This article is available online at <http://molpharm.aspetjournals.org>

ABSTRACT

2-Methoxyestradiol (2-MEO), a metabolite of estrogen, is an attractive lead compound for the development of novel antitumor and anti-inflammatory agents, because it embodies antiproliferative and antiangiogenic activities in one molecule. However, the affinity of 2-MEO for the estrogen receptor would lead to undesirable side effects. As a prelude to the design of 2-MEO-like compounds with an optimal activity profile, we assayed 2-MEO and a series of analogs for their ability to cause G₁ cell-cycle arrest (by measuring inhibition of DNA synthesis in human cultured airway smooth muscle) and to inhibit binding of [³H]estradiol at the estrogen receptor (ER; from rat uterine smooth muscle). One compound, a diacetoxymethoxy derivative, was identified with reasonable potency for DNA synthesis (pIC₅₀ = 5.97) but showed negligible affinity for the ER (pIC₅₀ < 5). Three-dimensional quantitative structure-activity relationships

were developed for these activities using comparative molecular field analysis (CoMFA) techniques. Comparison of optimized CoMFA models revealed distinct structural requirements for DNA synthesis inhibition and ER binding. For example, DNA synthesis inhibition is enhanced by electropositive substitutions in the 2-position below the plane of the steroid A-ring, whereas ER binding is favored by electronegative substitution in this position. Similarly, DNA synthesis inhibition correlates negatively with increased steric bulk in regions clustered around the A and B rings; changes in steric bulk in these regions has little correlation with ER binding. These observations will guide the design of new analogs with improved potency for desired characteristics (e.g., DNA synthesis inhibition) with minimal unwanted activities (e.g., ER binding).

Interest in the metabolites of estrogen has grown in the last decade, because it has been appreciated that a number of the actions of this sex hormone may be caused by biologically active metabolites. For example, the glucuronides of estrogen and its metabolites cause cholestatic jaundice (Zhu et al., 1996), whereas the catecholestrogens are implicated in the association between estrogen and increased incidence of certain tumors (Zhu and Conney, 1998). The cardioprotective effects of estrogen have been ascribed to an interaction between estrogen and the high-affinity estrogen receptor (ER); recent evidence suggests that the cardioprotective effects of estrogen are mediated largely, if not exclusively, via the

ER α subtype (Brouchet et al., 2001; Hodgin et al., 2001). Alternative lower affinity receptors that bind estrogen have been described, but these do not seem to interact with physiological levels of estrogen, opening up the possibility that a related ligand binds and activates these receptors under physiological conditions (Eriksson et al., 1980). 2-Methoxyestradiol (2-MEO, compound **1**; Table 1), once regarded as an inactive metabolite of estrogen, has been identified as an inhibitor of the proliferation of a variety of cell types and as an antiangiogenic and antitumor agent (Fotsis et al., 1994). Inhibition of smooth muscle proliferation by 2-MEO has given rise to suggestions that this or related compounds may have therapeutic applications in atherosclerosis (Nishigaki et al., 1995) and asthma (Stewart et al., 1999b), whereas regulatory effects of 2-MEO on lymphocytes and leukocytes provide a case for its use to treat rheumatoid arthritis (Jo-

This work was supported in part by AMRAD Operations Ltd, the National Health and Medical Research Council of Australia, Cryptopharma Pty Ltd, and contract NO1-CM67260 from the National Cancer Institute.

ABBREVIATIONS: ER, estrogen receptor; 2-MEO, 2-methoxyestradiol; CoMFA, comparative molecular field analysis; 3D-QSAR, three-dimensional quantitative structure-activity relationship; THF, tetrahydrofuran; CIMS, chemical ionization mass spectrometry; DMEM, Dulbecco's modified Eagle's medium; FCS, fetal calf serum; DMF, dimethyl formamide; PBS, phosphate buffered saline; PLS, partial least squares.

sefsson and Tarkowski, 1997). Furthermore, cytotoxic and antiangiogenic actions of 2-MEO on various tumor cell lines indicate that this agent has potential as an antitumor agent (Lottering et al., 1992; Fotsis et al., 1994; Cushman et al., 1995; Hamel et al., 1996; Cushman et al., 1997).

2-MEO has been evaluated for its antitumor potential in murine models of tumor growth, including immunodeficient mice bearing human tumor xenografts. Oral doses of 50 to 150 mg/kg have shown efficacy against murine angiosarcoma (Arbiser et al., 1999), murine Meth A sarcoma, and B16 melanoma (Fotsis et al., 1994). Furthermore, in immunodeficient mice, the growth of human pancreatic carcinoma (Schumacher et al., 1999) and human breast carcinoma [MDA-MB-435 (Klauber et al., 1997)] are reduced as a result of treatment with 2-MEO.

The precise mechanisms underlying the various actions of 2-MEO have not been elucidated. 2-MEO inhibits the depolymerization of microtubules and also retards the formation of polymeric tubulin, giving characteristics that overlap with those of both paclitaxel (Taxol) and colchicine (D'Amato et al., 1994; Hamel et al., 1996; Wang et al., 2000). It seems likely that tubulin binding and consequent inhibition of mitotic spindle function explains part of the antiproliferative action of 2-MEO. However, we and others have described an inhibitory effect of 2-MEO on cell-cycle progression to S-phase through G₁, as inferred from the inhibition of DNA synthesis in smooth muscle and in some other cell types (Nishigaki et al., 1995; Stewart et al., 1999b, 2001). This effect does not seem to be explained by microtubule actions, because it is not mimicked by either paclitaxel or colchicine (T. Harris and A. G. Stewart, unpublished observations). The extent to which suppression of DNA synthesis rather than microtubule dysfunction explains the potentially desirable in vivo activities of 2-MEO is uncertain. However, it is clear that in most circumstances of the predicted therapeutic use of 2-MEO, affinity for high-affinity ERs would be undesirable.

In the present study, we have examined the ability of 2-MEO and a series of analogs to inhibit DNA synthesis in smooth muscle cells and to bind to high affinity ER in rat uterine cytosol. We then used the technique of comparative molecular field analysis (CoMFA) to generate models describing three-dimensional quantitative structure activity relationships (3D-QSARs) for these two activities. The marked differences between the respective models suggest that there are distinct structural requirements for DNA synthesis inhibition and ER binding. The models should be valuable for guiding the synthesis of compounds showing increased DNA synthesis inhibitory activity without significant affinity for ER.

TABLE 1

Effect of 2-MEO on [³H]thymidine incorporation in the presence and absence of the mitogen thrombin

Data represent the mean and S.E.M. of four replicate incubations of one experiment that is representative of at least 13 different donors.

Incubation	[³ H]Thymidine Incorporation
Control	1298 ± 97
Thrombin 0.3 U/ml	3959 ± 468*
Thrombin + 2MEO (10 μM)	1082 ± 104

* *P* < 0.05, unpaired *t* test compared with control.

Compounds

Compounds used in this study are shown in Tables 4, 5, and 6. The syntheses of compounds **1**, **2**, **4**, **9** to **12**, **26** (Cushman et al., 1995), **5**, **18** (Cushman et al., 1997), **21**, **22** (Verdier-Pinard et al., 2000), and **23** to **31** (Wang et al., 2000) have been described previously. Compounds **3**, **16**, **18**, **19**, and **34-39** were purchased from Sigma (St. Louis, MO). ICI 182,780 (**17**) was purchased from Sapphire Bioscience (Alexandria, NSW, Australia). The syntheses of additional new compounds used in this study are described below.

Synthesis of 3,17β-O-Bis(methoxymethyl)estradiol (40). A solution of estradiol (**16**) (10.0 g, 36.7 mmol) in anhydrous tetrahydrofuran (THF, 80 ml) containing diisopropylethylamine (70 ml, 401 mmol) was stirred at 0°C under argon for 0.5 h. Methoxymethyl chloride (25 g, 310 mmol) was introduced and the resulting reaction mixture stirred at 60°C for 8 h. The reaction mixture was cooled to room temperature, poured into ice water (300 ml), and extracted with ethyl acetate (3 × 200 ml). The ethyl acetate layers were washed with saturated aqueous sodium bicarbonate (150 ml) and brine (2 × 100 ml), combined, dried over sodium sulfate, and evaporated to dryness. Chromatography of the residue (silica gel 230–400 mesh, ethyl acetate/hexane 1:8 by volume) gave compound **40** as a colorless oil (11.7 g, 88.4%): ¹H NMR (CDCl₃) δ 7.20 (d, *J* = 8.5 Hz, 1 H), 6.82 (dd, *J* = 8.5 and 2.6 Hz, 1 H), 6.77 (d, *J* = 2.6 Hz, 1 H), 5.14 (s, 2 H), 4.65 (d, *J* = 1.2 Hz, 2 H), 3.61 (t, *J* = 8.3 Hz, 1 H), 3.47 (s, 3 H), 3.37 (s, 3 H), 2.83 (m, 2 H), 2.15 (m, 5 H), 1.85 (m, 1 H), 1.40 (m, 7 H), 0.81 (s, 3 H).

Synthesis of 2-Formyl-3,17β-O-bis(methoxymethyl)estradiol (41). *Sec*-BuLi (1.3 M in cyclohexane, 100 ml, 130 mmol) was added dropwise to a solution of **40** (12.2 g, 33.8 mmol) in anhydrous THF (200 ml) at -78°C under argon and the resulting mixture was stirred at that temperature for 2.5 h. Anhydrous dimethylformamide (DMF; 20 ml, 255 mmol) was introduced dropwise and the resulting reaction mixture was stirred from -78°C to room temperature for 3 h. The reaction mixture was poured into an ice/water mixture (200 ml) and acetic acid (20 ml). The product was extracted with ethyl acetate (3 × 150 ml) and the ethyl acetate layers were washed with saturated aqueous sodium bicarbonate (150 ml) and brine (2 × 150 ml), combined, dried over sodium sulfate, and evaporated to dryness. Chromatography of the residue (silica gel 230–400 mesh, ethyl acetate/hexane 1:6 by volume) gave compound **41** as a colorless oil (11 g, 87%), which solidified after standing at room temperature overnight: m.p. 89 to 92°C. ¹H NMR (CDCl₃) δ 10.46 (s, 1 H), 7.80 (s, 1 H), 6.94 (s, 1 H), 5.29 (s, 2 H), 4.83 (ABq, *J* = 7.2 Hz, Δ*ν* = 3.4 Hz, 2 H), 3.64 (t, *J* = 8.5 Hz, 1 H), 3.54 (s, 3 H), 3.40 (s, 3 H), 2.84 (m, 2 H), 2.42–1.15 (m, 13 H), 0.81 (s, 3 H); CIMS (isobutane) *m/z* (relative intensity) 445 (MH⁺, 22), 389 (100). Analysis calculated for C₂₃H₃₂O₅: C, 71.11; H, 8.19. Found: C, 71.07; H, 8.48.

Synthesis of 2-Formylestradiol (42). A solution of compound **41** (370 mg, 0.95 mmol) and lithium tetrafluoroborate (1.8 g, 20 mmol) in acetonitrile (15 ml) containing water (1 ml) was heated at 72°C under nitrogen for 5 h. The reaction mixture was cooled to room temperature, poured into ice-cooled water (50 ml), and extracted with ethyl acetate (3 × 30 ml). The ethyl acetate layers were washed with brine (2 × 30 ml), dried over sodium sulfate, and evaporated to

TABLE 2

Effect of 2-MEO on cell number and viability in the presence and absence of the mitogen thrombin

Data represent the mean and S.E.M. of the number of cells/well of a six-well plate from four experiments, each in a culture from a different donor.

Incubation	Cell Number (× 10 ⁻⁴)	Nonviable Cells %
Control	28.5 ± 1.9	3.4 ± 0.5
2-MEO (10 μM)	31.1 ± 6.4	2.9 ± 0.5
Thrombin (0.3 U/ml)	37.6 ± 4.1	6.5 ± 0.8
Thrombin + 2-MEO (10 μM)	31.6 ± 3.3	6.0 ± 0.6

dryness. Chromatography of the residue with 10% ethyl acetate in hexane gave the desired product **42** (200 mg, 70%), which was crystallized from ethanol to afford a white crystalline solid: m.p. 236 to 237°C literature m.p. 230–232°C (Cushman et al., 1995). ¹H NMR (CDCl₃) δ 9.91 (s, 1 H), 7.58 (s, 1 H), 6.66 (s, 1 H), 3.68 (t, *J* = 8.4 Hz, 1 H), 2.88 (m, 2 H), 2.40 (m, 1 H), 2.18 (m, 1 H), 2.10–1.15 (m, 11 H), 0.79 (s, 3 H).

Synthesis of 2-Hydroximinomethylestradiol (13). Under nitrogen, hydroxylamine hydrochloride (1.1 g, 16 mmol) was added to a solution of compound **42** (240 mg, 0.8 mmol) in pyridine (10 ml). The resulting mixture was stirred and heated at 90°C for 1 h. The pyridine was removed under reduced pressure at 30 to 35°C and the residue was dissolved in an ethyl acetate (60 ml) and water (50 ml) mixture. The ethyl acetate solution was washed with water (30 ml) and brine (30 ml), dried over sodium sulfate, and evaporated to dryness. Chromatography of the residue on a silica gel column using 15% ethyl acetate in methylene chloride gave compound **13** (185 mg, 73%), which crystallized from ethyl acetate-methylene chloride to afford a white solid: m.p. 268 to 270°C. ¹H NMR (CDCl₃) δ 8.17 (s, 1 H), 7.13 (s, 1 H), 6.58 (s, 1 H), 4.86 (s, 2 H, OH), 3.66 (t, *J* = 8.3 Hz, 1 H), 2.81 (m, 2 H), 2.35–1.1 (m, 14 H), 0.77 (s, 3 H); CIMS (isobutane) *m/z* (relative intensity) 316 (MH⁺, 100). Analysis calculated for C₁₉H₂₅O₃N: C, 72.35; H, 7.99; N, 4.44. Found: C, 72.18; H, 8.22; N, 4.35.

Synthesis of 2-Methoximinomethylestradiol (14). Methoxyamine hydrochloride (1.1 g, 16 mmol) was added to a solution of compound **42** (100 mg, 0.8 mmol) in pyridine (5 ml) under nitrogen. The resulting mixture was stirred and heated at 90°C for 2 h. The pyridine was removed under reduced pressure at 30 to 35°C and the residue was dissolved in ethyl acetate (50 ml) and water (50 ml). The ethyl acetate solution was washed with water (30 ml) and brine (30 ml), dried over sodium sulfate, and evaporated to dryness. Chromatography of the residue on a silica gel column using 15% ethyl acetate in methylene chloride gave compound **14** (99 mg, 90%), which crystallized from ethyl acetate-methylene chloride to afford a white solid: m.p. 165 to 166°C; ¹H NMR (CDCl₃) δ 9.61 (s, 0.4 H), 8.11 (s, 0.6 H), 7.03 (s, 1 H), 6.71 (s, 1 H), 3.97 (s, 2 H, OH), 3.72 (t, *J* = 8.3 Hz, 1 H), 2.82 (m, 2 H), 2.35–1.1 (m, 16 H), 0.79 (s, 3 H); CIMS (isobutane) *m/z* (relative intensity) 330 (MH⁺, 100), 312 (MH⁺-H₂O, 40). Analysis calculated for C₂₀H₂₇O₆N·1/6 H₂O: C, 72.26; H, 8.28; N, 4.21. Found: C, 72.13; H, 8.38; N, 4.19.

Synthesis of 2-Formylestradiol Hydrazone (15). Hydrazine dihydrochloride (594 mg, 16 mmol) was added to a solution of compound **42** (85 mg, 0.8 mmol) in pyridine (5 ml) under nitrogen. The resulting mixture was stirred and heated at 90°C for 2 h. The pyridine was removed under reduced pressure at 30 to 35°C and the residue was suspended in a mixture of ethyl acetate (50 ml) and saturated aqueous NaHCO₃ (50 ml). The yellow solid was collected, washed with water and ethyl acetate, and dried under vacuum. Recrystallization from THF-methylene chloride gave compound **15** (62 mg, 70%): m.p. 340°C. ¹H NMR (CDCl₃) δ 10.9 (s, 0.4 H), 8.89 (s, 0.6 H), 7.53 (s, 1 H), 6.65 (s, 1 H), 3.54 (t, *J* = 8.3 Hz, 1 H), 2.81 (m, 2 H), 2.35–1.1 (m, 17 H), 0.69 (s, 3 H).

TABLE 3

Effects of thrombin and 2-MEO on cell-cycle distribution of human airway smooth muscle cells (*n* = 13).

Data are presented as mean ± S.E.M. (*n* = 13).

Incubation	Cell Cycle Distribution		
	G ₀ /G ₁	S	G ₂ /M
	%		
Control	77 ± 3	9 ± 2	14 ± 2
Thrombin (0.3 U/ml)	69 ± 3*	16 ± 3*	15 ± 1
Thrombin (0.3 U/ml) + 2-MEO (10 μM)	69 ± 4*	9 ± 2†	22 ± 3*†

* *P* < 0.05 by Bonferroni post hoc test compared with corresponding value in control incubation.

† *P* < 0.05 Bonferroni post hoc test thrombin + 2-MEO compared with thrombin.

Synthesis of 17β-Acetoxy-2-ethoxy-3-hydroxy-6-hydroximi-noestra-1,3,5(10)-triene (8). A solution of compound **43** (Cushman et al., 1997) (800 mg, 1.93 mmol) in pyridine (12 ml) was treated with hydroxylamine hydrochloride (1.07 g, 15.4 mmol). The resulting mixture was stirred and heated at 100°C for 30 min. The mixture was cooled to room temperature and then poured into ice water (150 ml). The compound was extracted with ethyl acetate (3 × 100 ml). The organic layers were washed with sodium bicarbonate (100 ml), water (2 × 100 ml), and brine (2 × 100 ml), dried over sodium sulfate and evaporated to dryness. Chromatography of the residue on a silica gel column using 30% ethyl acetate in hexane gave compound **8** (763 mg, 89%), which was crystallized from ethyl acetate-hexane to afford yellow crystals: m.p. 226 to 227°C. ¹H NMR (CDCl₃) δ 7.47 (s, 1 H), 6.75 (s, 1 H), 4.69 (t, *J* = 8.5 Hz, 1 H), 4.12 (q, *J* = 6.9 Hz, 2 H), 3.17 (dd, *J* = 4.3 and 18 Hz, 1 H), 2.40–1.20 (m, 14 H), 2.05 (s, 3 H), 1.43 (t, *J* = 6.9 Hz, 3 H), 0.85 (s, 3 H); CIMS (isobutane) *m/z* (relative intensity) 388 (MH⁺, 100), 372 (MH-H₂O, 10), 328 (75). Analysis calculated for C₂₂H₂₉O₅N: C, 68.20; H, 7.54; N, 3.61. Found: C, 68.04; H, 7.62; N, 3.54.

Synthesis of B-Homo-6-aza-2-ethoxy-3,17β-dihydroxyestra-1,3,5(10)-triene-6-one (44). A solution of compound **8** (700 mg, 1.63 mmol) in pyridine (10 ml) was treated with tosyl chloride (686 mg, 3.6 mmol) at room temperature. The resulting mixture was stirred for 2 h and the pyridine was removed in vacuo at ambient temperature to afford the crude oxime tosylate as a residue that was used without further purification. The residue was dissolved in a minimum amount of 40% chloroform in benzene (5 ml) and the material was applied to the top of a basic alumina column (30 × 3.5 cm). The column was eluted with chloroform-benzene (40 to 90% chloroform) and then allowed to stand overnight. The column was washed with methanol (200 ml) and 80% methanol in water (200 ml). The methanol eluate was collected and then evaporated to dryness. Chromatography of the residue on a silica gel column using ethyl acetate gave the ring-expanded lactam **44** (267 mg, 47%), which was crystallized from ethyl acetate to afford white crystals: m.p. 222 to 223°C. IR (KBr) 3336, 2931, 1661, 1514, 1469, 1440, 1371, 1320, 1243, 1119, 1046 cm⁻¹; ¹H NMR (CDCl₃) δ 7.31 (brs, 1 H), 6.74 (s, 1 H), 6.58 (s, 1 H), 4.12 (q, *J* = 6.7 Hz, 2 H), 3.75 (t, *J* = 8.5 Hz, 1 H), 2.41 (m, 2 H), 2.15–1.22 (m, 13 H), 1.44 (t, *J* = 7 Hz, 3 H), 0.82 (s, 3 H); CIMS (isobutane) *m/z* (relative intensity) 346 (MH⁺, 100), 328 (MH-H₂O, 20). Analysis calculated for C₂₀H₂₇O₄N·1/3 H₂O: C, 68.35; H, 7.93; N, 3.98. Found: C, 68.25; H, 8.03; N, 3.82.

Synthesis of B-homo-6-aza-2-ethoxy-3,17β-dihydroxyestra-1,3,5(10)-triene (45). A solution of borane in THF (1.0 M, 5.6 ml, 5.6 mmol) was added dropwise by syringe to a solution of compound **44** (97.8 mg, 0.28 mmol) in THF (5 ml) under argon at room temperature. The resulting solution was stirred for 6 h and then at gentle reflux for 4 h. The mixture was cooled and 6 N hydrochloric acid (2 ml) was added slowly through a pipette. The solvent was removed under reduced pressure and the residue was dissolved in ethyl acetate (60 ml). The ethyl acetate solution was washed with sodium bicarbonate (30 ml) and brine (2 × 20 ml), dried over sodium sulfate and evaporated to dryness. Chromatography of the residue on a silica gel column using 50% ethyl acetate in methylene chloride gave compound **45** (85 mg, 90%), which formed a white stable foam when it was evaporated from methylene chloride solution under reduced pressure. ¹H NMR (CDCl₃) δ 6.70 (s, 1 H), 6.28 (s, 1 H), 4.00 (q, *J* = 6.9 Hz, 2 H), 3.68 (t, *J* = 8.5 Hz, 1 H), 3.33 (t, *J* = 6.9 Hz, 1 H), 2.82 (t, *J* = 6.9 Hz, 1 H), 2.55 (dt, *J* = 8.5 and 2 Hz, 1 H), 1.20–2.20 (m, 15 H), 1.34 (t, *J* = 7.0 Hz, 3 H), 0.78 (s, 3 H); CIMS (isobutane) *m/z* (relative intensity) 332 (MH⁺, 100), 314 (MH-H₂O, 60). Analysis calculated for C₂₀H₂₉O₃N·1/4 H₂O: C, 71.50; H, 8.85; N, 4.14. Found: C, 71.64; H, 8.90; N, 4.29.

Synthesis of B-Homo-6-aza-3,17β,6a-triacetyl-2-ethoxyestra-1,3,5(10)-triene (46). Under nitrogen, acetic anhydride (1.83 g, 1.7 ml, 17.65 mmol) was added to a solution of compound **45** (146 mg, 0.44 mmol) in pyridine (5 ml). The resulting mixture was stirred at room temperature for 24 h and then poured into ice water (30 ml). The

compounds were extracted with ethyl acetate (3 × 50 ml) and the organic layers were washed with water (30 ml), saturated aqueous sodium bicarbonate (30 ml) and brine (30 ml), dried over sodium sulfate, and evaporated to dryness. Chromatography of the residue on a silica gel column using 33% ethyl acetate in methylene chloride gave compound **46** (169 mg, 84%), which formed a white stable foam when it was evaporated from ethyl acetate/hexane solution under reduced pressure: ¹H NMR (CDCl₃) δ 6.87 (s, 1 H), 6.78 (s, 1 H), 4.66 (t, *J* = 8.5 Hz, 1 H), 4.09 (q, *J* = 6.9 Hz, 2 H), 4.08 (t, *J* = 6.9 Hz, 1 H), 3.09 (m, 1 H), 2.46 (dt, *J* = 8.5 and 2 Hz, 1 H), 2.40 (s, 3 H), 2.28 (s, 3 H), 2.20–1.25 (m, 12 H), 1.93 (s, 3 H), 1.43 (t, *J* = 6.8 Hz, 3 H), 0.78 (s, 3 H); CIMS (isobutane) *m/z* (relative intensity) 458 (MH⁺, 100), 398 (35). Analysis calculated for C₂₆H₃₅O₆N: C, 68.25; H, 7.71; N, 3.06. Found: C, 68.36; H, 7.90; N, 3.43.

Synthesis of B-homo-6-aza-6-acetyl-2-ethoxy-3,17β-dihydroxyestra-1,3,5(10)-triene (47). A solution of compound **46** (150 mg, 0.33 mmol) in methanol (15 ml) was deoxygenated by bubbling a slow stream of nitrogen through it for 30 min. A similarly deoxygenated 1 M solution of sodium hydroxide in water (3.2 ml, 3.2 mmol) was added and the mixture was stirred at room temperature for 4.5 h. The reaction mixture was adjusted to pH 6–7 with acetic acid and the solvents were removed under reduced pressure. The residue was dissolved in ethyl acetate (60 ml) and the organic layer was washed with water (30 ml), saturated aqueous sodium bicarbonate (30 ml) and brine (30 ml), dried over sodium sulfate, and evaporated to dryness. Chromatography of the residue on a silica gel column using ethyl acetate gave compound **47** (105 mg, 86%), which crystallized from ethyl acetate-hexane to afford white crystals: m.p. 189 to 191°C. ¹H NMR (CDCl₃) δ 6.77 (s, 1 H), 6.67 (s, 1 H), 4.09 (q, *J* = 6.9 Hz, 2 H), 4.08 (t, *J* = 6.9 Hz, 1 H), 3.71 (t, *J* = 8.5 Hz, 1 H), 3.03 (m, 1 H), 2.40 (dt, *J* = 8.5 and 2.0 Hz, 1 H), 2.12–1.15 (m, 14 H), 1.87 (s, 3 H), 1.43 (t, *J* = 7.2 Hz, 3 H), 0.78 (s, 3 H); CIMS (isobutane) *m/z* (relative intensity) 374 (MH⁺, 100). Analysis calculated for C₂₂H₃₁O₄N·1/3 H₂O: C, 69.75; H, 8.41; N, 3.69. Found: C, 69.65; H, 8.25; N, 3.87.

Synthesis of B-Homo-6-aza-2-ethoxy-6a-ethyl-3,17β-dihydroxyestra-1,3,5(10)-triene (32). A solution of borane in THF (1.0 M, 4.8 ml, 4.8 mmol) was added dropwise by syringe under argon at room temperature to a solution of compound **47** (90 mg, 0.24 mmol) in THF (5 ml), and the resulting solution was stirred for 4 h and then at gentle reflux for 4 h. The mixture was cooled to room temperature and 6 N hydrochloric acid (1 ml) was added slowly through a pipette. The solvent was removed under reduced pressure and the residue was neutralized with saturated aqueous sodium bicarbonate solution and then extracted with ethyl acetate (3 × 30 ml). The ethyl acetate layers were washed with brine (2 × 30 ml), dried over sodium sulfate and evaporated to dryness. Chromatography of the residue on a silica gel column using 20% ethyl acetate in methylene chloride gave compound **32** (70 mg, 81%), which was converted into a white stable foam when it was evaporated from ethyl acetate-hexane solution under reduced pressure: ¹H NMR (CDCl₃) δ 6.68 (s, 1 H), 6.51 (s, 1 H), 5.51 (s, 1 H), 4.07 (q, *J* = 6.9 Hz, 2 H), 3.78 (t, *J* = 8.5 Hz, 1 H), 3.38 (td, *J* = 11.5 and 2.2 Hz, 1 H), 3.20 (qd, *J* = 12.6 and 7.1 Hz, 1 H), 2.94 (qd, *J* = 11.7 and 6.8 Hz, 1 H), 2.75 (td, *J* = 11.5 and 2.2 Hz, 1 H), 2.55 (dt, *J* = 8.5 and 2 Hz, 1 H), 2.20–1.20 (m, 16 H), 1.42 (t, *J* = 6.4 Hz, 3 H), 0.84 (s, 3 H); CIMS (isobutane) *m/z* (relative intensity) 360 (MH⁺, 100), 342 (MH-H₂O, 50). Analysis calculated for C₂₂H₃₃O₃N·1/6 H₂O: C, 72.96; H, 9.27; N, 3.86. Found: C, 72.97; H, 9.27; N, 3.85.

Synthesis of 3,17β-Diacetoxy-2-ethoxyestra-1,3,5(10),6-tetraene-6-yl Triflate (48). A stirred solution of compound **43** (Cushman et al., 1997) (1.0 g, 2.4 mmol) and 2,6-di-*tert*-butyl-4-methylpyridine (743 mg, 3.6 mmol) in dry methylene chloride (48 ml) was treated with triflic anhydride (0.52 ml, 3.12 mmol) dropwise under argon at 0°C and stirring was continued for 3 h at 0°C. The mixture was poured into ice water (200 ml) and extracted with ethyl acetate (3 × 100 ml). The combined organic layer was washed with 2 N HCl (4 ml) in water (50 ml) and then brine (3 × 100 ml) until neutral, dried over sodium sulfate, and evaporated to dryness. Chromatogra-

phy of the residue on a silica gel column using 20% ethyl acetate in hexane gave compound **48** (1.15 g, 90%), which crystallized from ethyl acetate-hexane to afford white crystals: m.p. 148 to 150°C. ¹H NMR (CDCl₃) δ 7.03 (s, 1 H), 6.88 (s, 1 H), 5.78 (s, 1 H), 4.71 (t, *J* = 8.5 Hz, 1 H), 4.09 (q, *J* = 6.9 Hz, 2 H), 2.51–1.36 (m, 11 H), 2.29 (s, 3 H), 2.05 (s, 3 H), 1.35 (t, *J* = 6.0 Hz, 3 H), 0.82 (s, 3 H); CIMS (isobutane) *m/z* (relative intensity) 547 (MH⁺, 100). Analysis calculated for C₂₅H₂₉O₈F₃S·1/2 ethyl acetate: C, 54.94; H, 5.63; F, 9.65. Found: C, 55.24; H, 5.39; F, 9.43.

Synthesis of 3,17β-Diacetoxy-2-ethoxy-7-hydroxy-6-oxoestra-1,3,5(10)-triene (6). A solution of chromium trioxide (484 mg, 4.84 mmol) on 90% glacial acetic acid (10 ml) was added dropwise at 12 to 15°C to a solution of compound **43** (500 mg, 1.21 mmol) in glacial acetic acid (15 ml). The resulting mixture was stirred at 12 to 15°C for 3 h. The mixture was poured into an ice/water mixture (150 ml) and the product was extracted with ethyl acetate (3 × 100 ml). The combined organic layer was washed with water (2 × 100 ml), sodium bicarbonate (2 × 100 ml) and brine (2 × 100 ml), dried over sodium sulfate and evaporated to dryness. Chromatography of the residue on a silica gel column using 30% ethyl acetate in hexane gave compound **6** (185 mg, 36%), which was crystallized from ethyl acetate-hexane to afford yellow crystals: m.p. 188 to 190°C. ¹H NMR (CDCl₃) δ 7.75 (s, 1 H), 6.95 (s, 1 H), 4.75 (t, *J* = 8.5 Hz, 1 H), 4.10 (q, *J* = 6.9 Hz, 2 H), 2.71 (q, *J* = 4 Hz, 1 H), 1.30–2.41 (m, 19 H), 0.82 (s, 3 H); CIMS (isobutane) *m/z* (relative intensity) 431 (MH⁺, 100), 413 (MH-H₂O, 50). Analysis calculated for C₂₄H₃₀O₇: C, 66.96; H 7.02. Found: C, 66.92; H 6.90.

Synthesis of 3,17β-Diacetoxy-2-ethoxyestra-1,3,5(10),6-tetraene (33). Under argon, 96% formic acid (0.31 ml, 8 mmol) was added to a stirred solution of compound **48** (1.1 g, 2.07 mmol), palladium acetate (18 mg, 0.08 mmol), triphenylphosphine (42 mg, 0.16 mmol), and triethylamine (1.68 ml, 12 mmol) in anhydrous DMF (8 ml). The mixture was stirred for 3 h at 60 to 62°C and then cooled to room temperature, diluted with brine (100 ml), and extracted with ethyl acetate (3 × 100 ml). The organic layers were washed with brine (3 × 100 ml), dried over sodium sulfate and evaporated to dryness. Chromatography of the residue on a silica gel column using 20% ethyl acetate in hexane provided compound **33** (0.75 g, 89%), which was crystallized from ethyl acetate-hexane to afford white crystals: m.p. 158 to 159°C. ¹H NMR (CDCl₃) δ 6.87 (s, 1 H), 6.71 (s, 1 H), 6.37 (d, *J* = 9.8 Hz, 1 H), 5.82 (d, *J* = 9.8 Hz, 1 H), 4.71 (t, *J* = 8.5 Hz, 1 H), 4.09 (q, *J* = 6.9 Hz, 2 H), 2.51–1.36 (m, 11 H), 2.28 (s, 3 H), 2.06 (s, 3 H), 1.37 (t, *J* = 6.9 Hz, 3 H), 0.82 (s, 3 H); CIMS (isobutane) *m/z* (relative intensity) 399 (MH⁺, 100). Analysis calculated for C₂₄H₃₀O₅: C, 72.34; H, 7.59. Found: C, 72.45; H, 7.60.

Synthesis of 3,17β-Diacetoxy-2-ethoxy-7α-hydroxyestra-1,3,5(10)-triene-6α-(*m*-chlorobenzoate) (49) and 3,17β-Diacetoxy-2-ethoxy-7α-hydroxyestra-1,3,5(10)-triene-6β-(*m*-chlorobenzoate) (50). A solution of *m*-chloroperbenzoic acid (260 mg, 57 to 81%, 0.86–1.23 mmol) in methylene chloride (10 ml) was added dropwise to a stirred solution of compound **33** (343 mg, 0.86 mmol) in methylene chloride (20 ml) under nitrogen atmosphere at 0°C. The mixture was allowed to come to room temperature and stirred for 20 h. The mixture was poured into ice-cold saturated sodium bicarbonate (100 ml) and the mixture was extracted with methylene chloride (3 × 50 ml). The combined organic layer was washed with water (2 × 50 ml), sodium bicarbonate (2 × 50 ml) and brine (2 × 50 ml), dried over sodium sulfate, and evaporated to dryness. Chromatography of the residue on a silica gel column using 25% ethyl acetate in hexane gave compound **49** (153 mg, 31%), which was crystallized from diethyl ether to afford a white solid: m.p. > 110°C (dec); ¹H NMR (CDCl₃) δ 8.08 (s, 1 H), 8.00 (d, *J* = 7.8 Hz, 1 H), 7.57 (d, *J* = 7.8 Hz, 1 H), 7.40 (t, *J* = 7.8 Hz, 1 H), 6.91 (s, 1 H), 6.87 (s, 1 H), 6.19 (d, *J* = 3.5 Hz, 1 H), 4.72 (t, *J* = 8.5 Hz, 1 H), 4.24 (d, *J* = 3.7 Hz, 1 H), 4.01 (q, *J* = 6.9 Hz, 2 H), 2.88 (bs, 1 H), 2.24 (s, 3 H), 2.04 (s, 3 H), 2.04–1.30 (m, 11 H), 1.36 (t, *J* = 6.9 Hz, 3 H), 0.83 (s, 3 H). Compound **50** (260 mg, 53%) was crystallized from ethyl acetate-hexane to afford a white solid: m.p. 140–145°C. ¹H NMR (CDCl₃) δ 8.0 (s, 1 H),

7.84 (d, $J = 7.8$ Hz, 1 H), 7.50 (d, $J = 7.8$ Hz, 1 H), 7.35 (t, $J = 7.8$ Hz, 1 H), 7.01 (s, 1 H), 6.94 (s, 1 H), 5.90 (d, $J = 2.2$ Hz), 4.72 (t, $J = 8.5$ Hz, 1 H), 4.06 (q, $J = 6.9$ Hz, 2 H), 4.02 (d, $J = 2.2$ Hz, 1 H), 2.71 (dt, $J = 4.2$ and 2.1 Hz, 1 H), 2.24 (s, 3 H), 2.05 (s, 3 H), 2.04–1.30 (m, 11 H), 1.37 (t, $J = 6.9$ Hz, 3 H), 0.83 (s, 3 H).

Synthesis of 2-Ethoxy-3,6 α ,7 α ,17 β -tetrahydroxyestra-1,3,5(10)-triene (51). A solution of LiAlH₄ in THF (1.0 M, 5 ml, 5 mmol) was added to a solution of compound **49** (270 mg, 0.49 mmol) in THF (10 ml) and the resulting suspension was stirred at gentle reflux overnight (14 h). The reaction mixture was cooled and added cautiously into ice/water (50 ml), and then acidified to pH 1 with 3 M HCl. The mixture was extracted with ethyl acetate (3 \times 60 ml). The organic layers were washed with water (50 ml), sodium bicarbonate (50 ml), and brine (50 ml), dried over sodium sulfate, and evaporated to dryness. Chromatography of the residue on a silica gel column using 30% acetone in methylene chloride gave compound **51** (141 mg, 88%), which was crystallized from ethyl acetate-methylene chloride to afford white crystals: m.p. 231 to 232°C. ¹H NMR (CDCl₃) δ 7.05 (s, 1 H), 6.82 (s, 1 H), 4.53 (d, $J = 3.7$ Hz, 1 H), 4.08 (q, $J = 6.9$ Hz, 2 H), 3.93 (d, $J = 3.8$ Hz, 1 H), 3.69 (t, $J = 8.5$ Hz, 1 H), 2.95 (m, 2 H), 2.68 (dt, $J = 7.6$ Hz and 4.0 Hz, 1 H), 2.34 (dd, $J = 10.0$ and 3.2 Hz, 1 H), 2.14–1.20 (m, 11 H), 1.35 (t, $J = 6.8$ Hz, 3 H), 0.78 (s, 3 H); CIMS (isobutane) m/z (relative intensity) 349 (MH⁺, 20), 331 (MH₂O, 100), 313 (MH⁺-2H₂O, 50). Analysis calculated for C₂₀H₂₈O₅-1/3 H₂O: C, 67.78; H, 8.15. Found: C, 67.76; H, 8.21.

Synthesis of 2-Ethoxy-3,6 β ,7 α ,17 β -tetrahydroxyestra-1,3,5(10)-triene (7). A solution of LiAlH₄ in THF (1.0 M, 5 ml, 5 mmol) was added to a solution of compound **50** (120 mg, 0.21 mmol) in THF (10 ml), and the resulting suspension was stirred at gentle reflux overnight (14 h). The reaction mixture was cooled and added cautiously into ice/water (50 ml) and then acidified to pH 1 with 3 M HCl. The mixture was extracted with ethyl acetate (3 \times 60 ml). The organic layers were washed with water (50 ml), sodium bicarbonate (50 ml) and brine (50 ml), dried over sodium sulfate, and evaporated to dryness. Chromatography of the residue on a silica gel column using 30% acetone in methylene chloride gave compound **7** (48 mg, 66%), which was crystallized from ethyl acetate/diethyl ether to afford white crystals: m.p. 182 to 184°C. ¹H NMR (CDCl₃) δ 6.84 (s, 1 H), 6.78 (s, 1 H), 4.34 (bs, 1 H), 4.09 (q, $J = 6.9$ Hz, 2 H), 3.86 (bs, 1 H), 3.71 (t, $J = 8.5$ Hz, 1 H), 2.95 (bs, 3 H, OH), 2.56 (dt, $J = 7.6$ and 4.0 Hz, 1 H), 2.34 (dd, $J = 9.9$ and 3.2 Hz, 1 H), 2.14–1.20 (m, 11 H), 1.38 (t, $J = 6.9$ Hz, 3 H), 0.78 (s, 3 H); CIMS (isobutane) m/z (relative intensity) 349 (MH⁺, 18), 331 (MH₂O, 100), 313 (MH⁺-2H₂O, 50). Analysis calculated for C₂₀H₂₈O₅-1/3 H₂O: C, 67.78; H, 8.15. Found: C, 67.52; H, 8.21.

Materials and Methods

Synthetic Chemistry

Melting points were determined in capillary tubes on a Mel-Temp apparatus and are uncorrected. Spectra were obtained as follows: ¹H NMR spectra were recorded on a Varian VXR-300S spectrometer (Palo Alto, CA) using tetramethylsilane as an internal standard; CIMS spectra were obtained on a Finnigan 4000 spectrometer (Thermo Finnigan, San Jose, CA); microanalyses were performed at the Purdue Microanalysis Laboratory. Flash column chromatography was performed on 60- μ m silica gel from Scientific Adsorbents, Inc. (Atlanta, GA). Most chemicals and solvents were analytical grade and used without further purification. Commercial reagents were purchased from Aldrich Chemical Company (Milwaukee, WI).

Culture of Human Airway Smooth Muscle

Human airway smooth muscle was cultured from macroscopically normal bronchi (0.5- to 2-cm diameter) obtained from lung resection or heart-lung transplant specimens provided by the Alfred Hospital (Melbourne) according to methods published in

detail previously (Fernandes et al., 1999; Stewart et al., 1999a). Approximately 0.1 g of smooth muscle was stripped from the wall of the bronchus for each cell culture. Dissected tissue was immersed in Dulbecco's modified Eagle's medium (DMEM; Flow Laboratories, Irvine, Scotland, UK), supplemented with 100 U/ml penicillin G (CSL Australia, Parkville, Victoria, Australia) and 100 μ g/ml streptomycin (CSL Australia). The tissue was rinsed in phosphate-buffered saline (PBS; Oxoid, Basingstoke, Hampshire, England) and the airway smooth muscle was chopped into 2-mm³ pieces and digested for 2 h in DMEM containing elastase (0.5 mg/ml; Worthington Biochemical, Freehold, NJ) followed by a 12-h incubation in DMEM containing collagenase (1 mg/ml) (Worthington Biochemical), at 37°C with agitation. The resulting cell suspension was centrifuged and washed three times with PBS. After the last centrifugation step, the cells were resuspended in 25 ml of DMEM supplemented with L-glutamine (2 mM; Sigma), penicillin G (100 U/ml), streptomycin (100 μ g/ml), amphotericin B (2 μ g/ml; Wellcome, Stevenage, UK) and heat-inactivated FCS (10% v/v; CSL Australia) and seeded into 25-cm² culture flasks. The primary isolates were incubated for 7 to 14 days to reach confluence. Cells were harvested weekly by 10 min exposure to trypsin (0.5%; CSL Australia) and EDTA (1 mM in PBS; BDH, Kilsyth, Victoria, Australia) and passaged at a 1:3 ratio into 75-cm² flasks.

Inhibition of DNA Synthesis

Cells were subcultured into 24-well plates in a 1:3 split ratio at a density of approximately 1.5×10^4 cells/cm² and grown to monolayer confluence in antimicrobial-supplemented DMEM containing 10% fetal calf serum, over a 72 to 96 h period (5% CO₂ in air, 37°C). Quiescence was induced 24 h before stimulation by removing the medium, washing with PBS and replacing the medium with serum-free DMEM (supplemented as described previously) to synchronize the cells in G₀ of the cell cycle. Cells were stimulated by the addition of thrombin [bovine plasma, 0.3 U/ml, prepared in PBS containing bovine serum albumin (0.25% w/v; Sigma). Monomed A (1% v/v; CSL Australia), a serum-free medium supplement containing insulin, transferrin, and selenium was added to all wells. 2-MEO and analogs were dissolved in 100% dimethyl sulfoxide (BDH, Poole, Dorset, UK) at a concentration of 10 mM and diluted serially in PBS, before addition of 100 μ l to 1 ml of medium overlying airway smooth muscle, up to a maximal final analog concentration of 10 μ M. This resulted in a final maximum concentration of 0.1% dimethyl sulfoxide, which was added to the corresponding control wells. Concentration-response relationships were constructed from an evaluation of the effects of the analogs (0.1 μ M to 10 μ M, in half-log increments) on thrombin-stimulated DNA synthesis. Individual responses were calculated by incubating cells with the analog agents for 24 h (5% CO₂ in air, 37°C) then pulsing the cells with [³H]thymidine (1 μ Ci/ml; Amersham, Little Chalfont, Buckinghamshire, UK) for 4 h to label newly synthesized DNA. Before harvest, the medium was removed and the cells were solubilized by the addition of 100 μ l sodium hydroxide (1 M; Selby Biolab, Melbourne, Australia) to each well. Cellular DNA was immobilized onto glass fiber filters using a Packard Filtermate 196 Cell Harvester (Packard BioSciences, Melbourne, Australia). The filters were washed three times with 3 ml distilled H₂O and 1 ml ethanol (100%). Packard Microscint-40 (Packard) was added to dried filters and radioactivity was measured using a Packard Top Count Microplate Scintillation Counter.

ER Binding Assay

ER affinity of estradiol (**16**), its metabolites [2-hydroxyestradiol (**19**), 2-MEO (**1**)] and analogs were determined using rat uterine cytosol as a source of ER (Markaverich and Clark, 1979). Uteri (6–10 per batch) were isolated from Brown Norway rats (250–350 g), washed free from blood in saline, and homogenized in 10 mM Tris buffer [pH 7.4, 1.5 mM EDTA, 10% (w/v) glycerol, 1 mM phenylm-

ethylsulfonylfluoride] using an Ultra Turrax homogenizer for 3 15-s bursts with intervals of 1 min on ice. For additional studies of ER in smooth muscle, cytosol from human airway smooth muscle was prepared from 16- × 175-cm² flasks of confluent cells grown as described, and serum-deprived for 24 h before harvest. The cells were washed 3 times with PBS before the addition of a total of 4 ml of the 10 mM Tris buffer described above. The cells were scraped from the plates and subjected to homogenization by 30 passes in a glass homogenizer. The airway smooth muscle and rat uterus preparations were then processed in the following manner. Nuclear material and cellular debris were removed by centrifugation at 750g at 4°C for 10 min (Sorvall RT7) and cytosol was prepared by centrifugation at 30,000g for 120 min at 4°C in a Beckman JM1 centrifuge. The cytosol was diluted to contain approximately 1 mg/ml protein (rat uterine extract) or 0.015 mg/ml (airway smooth muscle) determined using the Bradford method (Bio-Rad, Hercules, CA). Binding assays were carried out by overnight incubation at 4°C in 300 μl of the above described buffer: 200 μl of cytosol, 50 μl of displacer [10 mM estradiol (**16**) or buffer] and 50 μl of 0.2 nM [³H]estradiol. Separation of bound from free radioligand was achieved by the addition of 500 μl of dextran-coated charcoal (400 mg of dextran clinical grade C and 2 g of charcoal, Norit A in 100 ml of Tris buffer) and centrifugation at 4°C in a Sorval RT7 at 2000g for 10 min. Preliminary saturation analysis over the range 0.01 to 50 nM [³H]estradiol yielded a K_d and B_{max} values of 0.18 nM and 112 fmol/mg protein, respectively [$n = 3$, analysis using Prism (GraphPad Software, San Diego, CA)], indicating that the 0.2 nM concentration was suitable for displacement studies. Saturation analysis carried out on airway smooth muscle-derived cytosol revealed an affinity (K_D) of 0.53 nM and a much higher density of binding sites of 1071 fmol/mg protein. The very low yield of protein from large amounts of cultured airway smooth muscle made further analyses of ER binding in this cell type impractical. Analyses of 2-MEO (**1**) and analogs were initially carried out over the range 0.1 nM to 10 μM in decade increments and, after identification of the appropriate range, displacement of estradiol was determined using three to four concentrations per decade. The data were fitted to the Cheng and Prusoff equation using the K_d value of 0.18 nM (Prism) and the data are presented as pIC₅₀.

Cell Enumeration

Cells were seeded onto six-well plates at a density of 1.5×10^4 cells cm⁻², made quiescent as described previously, and then stimulated for 48 h with thrombin (0.3 U/ml). At the end of the 48 h incubation period, cells were detached from the culture plate by the addition of trypsin (0.5% w/v in PBS containing 1 mM EDTA), incubated for 5 min at ambient temperature in PBS containing 0.5% (w/v) trypan blue, washed twice (2% FCS in PBS), isolated by centrifugation (12,000g, 5 min) and resuspended in 200 μl 2% FCS in PBS for counting in a hemocytometer chamber.

Flow Cytometric Analyses of Cell Cycle Status

Cells seeded into 6-well plates at a density of 1.5×10^4 cells cm⁻² and made quiescent as described previously were then stimulated with thrombin (0.3 U/ml) for 48 h. Monomed A was added to all cells (including control cells) at the time of mitogen addition. Cells were detached from the culture plates by incubation with trypsin for 30 min at 37°C (0.5% w/v). The resulting suspension was washed in PBS twice before resuspension in 1 ml of 70% ethanol for storage for up to 3 weeks at -20°C. Before staining, cells were washed twice (2% FCS in PBS) to remove the ethanol. Fixed cells were stained with propidium iodide (50 μg/ml) in Triton X-100 (0.1% v/v) with RNase II (180 mU/ml). The cell suspension was passed through an 18-gauge needle to facilitate the separation of cell clumps. Cells were stored for 24 h before analysis. Cell cycle status was analyzed using a FACScan Instrument (BD, Franklin Lakes, NJ). Ten thousand events from each sample were counted and analyzed using a ModFitLT V2.0 analysis package (Verity Software House, Topsham, ME).

Statistical Analyses

All incubations for the [³H]thymidine incorporation assays were conducted in triplicate or quadruplicate. Experiments were carried out in at least three cell lines, each derived from at least three different individuals; results are expressed as the mean of these estimations. To minimize the influence of variability between tissue donors on comparisons of data, the response to thrombin in the presence of the antagonist was expressed as a percentage of the thrombin control in individual cultures (100%). The potency of the analogs was determined by fitting log concentration-response data using nonlinear regression to fit a sigmoidal relationship. The pIC₅₀ values represent the negative log of the concentrations that reduce the thrombin-stimulated DNA synthesis to 50% of the response in the absence of inhibitor. The binding data were analyzed by the Cheng and Prusoff equation (Prism) and are presented as pIC50 values that represent the log of the concentration of analog that displaces 50% of the specifically bound [³H]estradiol. The standard errors of these pIC50 values (Tables 4 to 6) did not exceed 5% of the mean value.

Molecular Modeling Studies

Molecular modeling studies were carried out using SYBYL software (version 6.4; Tripos Inc., St Louis, MO) running on a Silicon Graphics O2 workstation equipped with a 175-MHz R10000 processor (Silicon Graphics, Mountain View, CA).

Generation of Molecular Models. Molecular models of 2-MEO, its analogs, and other compounds used in this study were constructed from standard SYBYL fragments, and their geometry was optimized (Powell conjugate gradient minimization, termination at a gradient of $<0.005 \text{ kcal mol}^{-1} \text{ \AA}^{-1}$) using the Tripos forcefield and Gasteiger-Marsili partial atomic charges (Gasteiger and Marsili, 1980). Lowest energy conformations of flexible sidechains were identified by applying the Systematic Search routine in SYBYL to all rotatable bonds (10° torsion angle increments of flexible bonds) with reminimization, as described above, of low-energy candidates. Spectroscopic data of compound **6** was consistent with a degree of keto-enol tautomerism at the 6- and 7-positions; the compound was thus modeled as the enediol.

Calculation of CoMFA Fields. 3D-QSAR relationships for the compounds were generated using the CoMFA routines in the QSAR option in Sybyl (Cramer et al., 1988). Compounds were first aligned (see below) and steric and electrostatic energies calculated for each molecule throughout a 2-Å grid, extending 4 Å beyond the van der Waals' volume of all molecules, using an sp³ carbon atom probe with a charge of +1 and a distance-dependent dielectric constant. The resultant matrices—a row for each compound, a column of biological activities (either DNA synthesis inhibition or ER binding), and multiple columns for each molecule containing the molecular field strengths at each grid point—were subjected to partial least-squares (PLS) regression analysis (see below) to derive 3D-QSAR models.

Three-Dimensional Alignments for CoMFA. 3D-QSAR models obtained by CoMFA techniques are sensitive to the spatial alignment of the molecules under study. To examine the effect of alignment, CoMFA models were generated for the following alignments (created by aligning molecules with 2-MEO using the Fit routine in Sybyl):

Steroid alignments.

1. Aligned by overlaying the atoms corresponding to the three oxygen atoms in 2-MEO. These atoms are common to all analogs and, by analogy to the requirements for ER binding (Anstead et al., 1997), might therefore correspond to key pharmacophoric points.
2. Aligned as in 1, except that the side chain in position R2 was oriented to match the conformation of this group in 2-MEO, except for compounds with an acetate group in this position. These compounds had their side chains adjusted to the conformation of the side chain in 2-MEO, followed by minimization,

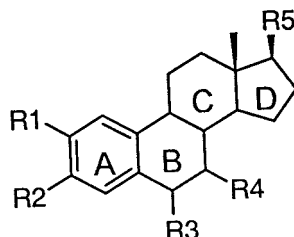
rather than in their strictly low energy conformations as in alignment 1. This alignment would be expected to reduce the likelihood that alternative side chain conformations (any of which might be reasonably accessible in a biological milieu)

could introduce inappropriate structural variation in compounds.

3. Aligned by fitting all common, nonhydrogen atoms. This alignment takes weight away from the positions of the oxygen atoms

TABLE 4

Structures of 2-methoxyestradiol (1) and analogs



	R1	R2	R3	R4	R5	Biological Activity (pIC ₅₀)	
						DNA Inhibition	ER Binding
1	CH ₃ O-	HO-	H-	H-	HO-	5.21	7.5
2	CH ₃ O-	BzlO-	H-	H-	BzlO-	<5	N.D.
3	CH ₃ O-	HO-	H-	H-	O=	stim ^a	4.97
4	CH ₃ CH ₂ O-	HO-	H-	H-	HO-	5.04	7.37
5	CH ₃ CH ₂ O-	HO-	O=	H-	HO-	5.72	5.45
6 ^b	CH ₃ CH ₂ O-	CH ₃ COO-	O=	HO-	CH ₃ COO-	5.97	<5
7	CH ₃ CH ₂ O-	HO-	HO	HO	HO-	<5	N.D.
8	CH ₃ CH ₂ O-	HO-	HO-N=	H-	CH ₃ COO-	5.99	N.D.
9	OHC-	HO-	H-	H-	HO-	<5	8.09
10	OHC-	BzlO-	H-	H-	BzlO-	<5	N.D.
11	CH ₃ CH ₂ -	HO-	H-	H-	HO-	4.98	8.98
12	CH ₃ CH ₂ S-	HO-	H-	H-	HO-	5.09	8.18
13	HO-N=CH-	HO-	H-	H-	HO-	5.95	9.16
14	CH ₃ O-N=CH-	HO-	H-	H-	HO-	5.24	7.61
15	NH ₂ -N=CH-	HO-	H-	H-	HO-	<5	N.D.
16	H-	HO-	H-	H-	HO-	<5	9.89
17	H-	HO-	H-	C ₂ F ₅ (CH ₂) ₃ S(0)(CH ₂) ₉ -	HO-	5.88	8.62
18	Br-	BzlO-	H-	H-	BzlO-	<5	N.D.
19	HO-	HO-	H-	H-	HO-	5.03	9.49
20	HO-	BzlO-	H-	H-	BzlO-	<5	N.D.

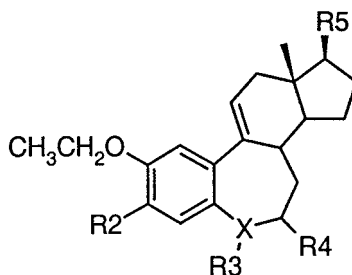
N.D., not determined.

^a Caused stimulation of DNA synthesis.

^b Modelled as the enediol (see *Methods*).

TABLE 5

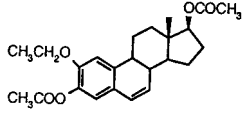
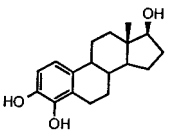
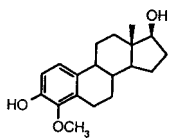
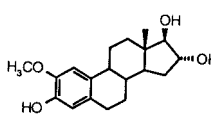
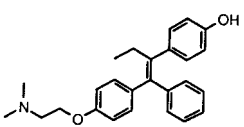
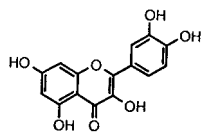
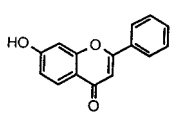
Analogues of 2-ethoxyestradiol (4) with a seven-membered B-ring.



	R2	R3	R4	R5	X	Biological Activity (pIC ₅₀)	
						DNA Inhibition	ER Binding
21	HO-	H-	H-	HO-	-C-	<5	<5
22	CH ₃ COO-	H-	H-	CH ₃ COO-	-C-	<5	<5
23	HO-	O=	H-	HO-	-C-	5.28	<5
24	CH ₃ COO-	O=	H-	HO-	-C-	5.00	<5
25	HO-	O=	H-	CH ₃ COO-	-C-	5.32	<5
26	CH ₃ COO-	O=	H-	CH ₃ COO-	-C-	5.52	<5
27	HO-	H-	O=	HO-	-C-	5.07	N.D.
28	HO-	HON=	H-	HO-	-C-	5.6	<5
29	HO-	H-	HON=	HO-	-C-	5.29	<5
30	HO-	CH ₃ ON=	H-	HO-	-C-	5.30	N.D.
31	CH ₃ COO-	CH ₃ ON=	H-	CH ₃ COO-	-C-	5.51	<5
32	HO-	CH ₃ CH ₂ -	H-	HO-	-N-	<5	N.D.

N.D., not determined.

TABLE 6
Additional compounds used in this study

Structure	Biological Activity (pIC ₅₀)	
	DNA Inhibition	ER Binding
	5.24	N.D.
	5.33	9.77
	<5	N.D.
	stim ^a	5.56
	<5	9.14
	<5	N.D.
	<5	N.D.

N.D., not determined.

^a Caused stimulation of DNA synthesis.

used in alignments 1 and 2 and places more emphasis on the positions of backbone atoms. Side chains were in their low energy conformations as in alignment 1. This alignment was thought to be worthy of examination, given that the estrogens are likely to be compounds that are well matched to the ER (Andrews et al., 1984).

4. Aligned as in 3, except that side chain conformations were adjusted to match those of 2.

Nonsteroid alignments.

- 4-OH-tamoxifen (**37**) was aligned by superimposing the centroids of two aromatic rings of **37** with the centroids of the A and D rings of 2-MEO and the aromatic O-substituents of **37** with the O-substituents of 2-MEO in positions R2 and R5. This alignment has previously been used in developing 3D-QSAR relationships for nonsteroidal ligands for the estrogen receptor (Sadler et al., 1998).
- Flavones (**38** and **39**) were aligned by superimposing the carbon atoms of the aromatic ring of the flavone α to the carbonyl group. The centroid of the other aromatic ring was fitted to the centroid of the steroid D-ring.

Partial Least Squares (PLS). PLS is a type of regression analysis particularly suited to situations such as CoMFA, where the independent variables (i.e., molecular field strengths) greatly outnumber the dependent variables (biological activities) (Wold, 1991). It uses a means of data reduction to transform the dependent and independent variables into a set of so-called principal components, which are mutually orthogonal descriptors from which the QSAR equations can subsequently be derived. The optimal number of components (after which the inclusion of additional components does not further improve the quality of the model) for the models for ER binding and DNA synthesis inhibition was determined in so-called cross-validated runs. In these runs, successive QSAR equations are generated in which one compound is omitted, and the model derived in the absence of this compound and used to predict the activity of the omitted compound. The process was repeated until equations had been derived with each compound omitted once—the activity of each omitted compound was predicted—giving a set of n QSAR equations for n compounds (leave-one-out method). The final CoMFA models were then derived from non-cross-validated runs using the optimal number of components determined from the cross-validated runs. The quality of the QSAR equations generated during the cross-validated runs was measured by the term q^2 (the cross-validated r^2), calculated thus: $q^2 = (SD - PRESS) / SD$, where SD is the variance of the biological activities, and PRESS is the sum of the squares of the differences between predicted and observed biological activities of each compound as it is left out of the analysis during the cross-validation process.

Because it involves the omission of data during its calculation, q^2 is an inherently conservative estimate of the predictivity of a model. It is generally accepted that q^2 values greater than 0.5—halfway between no model ($q^2 = 0.0$) and a perfect model ($q^2 = 1.0$)—are likely to be of useful predictive value.

To increase the speed of the cross-validated runs, CoMFA columns with a variance of less than 2.0 kcal/mol (minimum $\sigma = 2.0$) were excluded from PLS analyses; a minimum sigma σ value of 0.0 kcal/mol (i.e., no filtering) was used during non-cross-validated analyses, as recommended in the Tripos manual.

Optimization of CoMFA Models. The CoMFA implementation in Sybyl allows the user to optimize the model by altering several parameters.

- Choosing the cut-off value for the energy at a given grid point (grid points whose computed energy is greater than the cut-off value are assigned the cut-off value). The effect of cut-off on the quality and predictive capabilities of the CoMFA models was thus examined over a range of cut-off values (10–100 kcal/mol).
- Scaling the field strength data (implementing either CoMFA standard scaling, the default choice, which attempts to balance the potential influence of each field and column on the resulting QSAR by scaling the data to the overall field mean and standard deviation, or no scaling, which emphasizes variables with a greater numerical spread, typically those describing the steric field).
- Dropping electrostatic values at the steric maximum, (i.e., so that electrostatic field contributions from “inside” a molecule are not considered).

The effect of altering combinations of these parameters was examined systematically. Further optimization of models was carried out by examining the effects of removing “outlying” compounds. Two methods were used to define outliers: compounds whose residual was greater than three times the S.D. of the residual of the entire dataset and compounds which, when removed from the analysis, gave rise to CoMFA models with an improved q^2 values compared with that obtained with the compound present.

After the identification and removal of outlying compounds, the models were reoptimized with regard to cut-off, scaling, and dropping of electrostatics as described above, in an iterative fashion.

Default values were used for other settings. The pIC_{50} of compounds deemed to be inactive was set to 5, to reduce arbitrary skewing of the data.

Presentation of CoMFA Models. The final optimized CoMFA models for DNA inhibition and ER binding obtained from non-cross-validated runs are presented as isocontour maps of extreme values of the product of the S.D. and coefficients of the 3D-QSAR equations derived by PLS analysis at the grid points, after scaling of this product from 0 to 100%. (The product of the S.D. and coefficient was also used to obtain the relative contributions of the steric and electrostatic fields.) Such plots indicate where in space differences in either the steric or electrostatic fields of the molecules in the data set correlate most with differences in biological activity (Cramer et al., 1988). Generally, contours corresponding to >85% and <15% of the signal gave readily interpretable isocontour maps (i.e., regions associated with the molecular fields of the datasets that correlated either positively or negatively with biological activity were represented by clearly defined, discrete polyhedra), except for the electrostatic field map for DNA synthesis inhibition, where contours of >80% and <20% were used to give a clearer indication of the position of electrostatically and sterically favorable substituents.

Results

Synthetic Chemistry

Prior work has demonstrated that the cytotoxicities and tubulin polymerization inhibitory potencies of 2-MEO analogs can be modulated by replacement of the 2-methoxyl group by other substituents (Cushman et al., 1995, 1997). Replacement of the 2-methoxyl group of 2-MEO by 2-ethoxyl and 2-(*E*)-1-propenyl substituents resulted in compounds that were more potent than estradiol itself (Cushman et al., 1995). In general, the optimal substituent in the 2-position proved to be a straight chain containing three atoms from the second row of the periodic table. To investigate this in more detail, the oxime (**13**), methoxime (**14**), and hydrazone (**15**) derivatives were prepared as outlined in Scheme 1. Treatment of estradiol (**16**) with methoxymethyl chloride in the presence of diisopropylethylamine afforded the bis(methoxymethyl) ether **40**. Intermediate **40** was regioselectively lithiated in the 2-position with *sec*-butyllithium in THF, followed by formylation with DMF to yield the aldehyde **41** in high yield as a single regioisomer. Deprotection of the bis(methoxymethyl) ether **41** with lithium tetrafluoroborate in acetonitrile provided 2-formylestradiol (**42**) (Ireland and Varney, 1986). The oxime (**13**), methoxime (**14**), and hydrazone (**15**) derivatives were then obtained by reaction of **42** with hydroxylamine, methoxylamine, and hydrazine, respectively.

Certain B-ring expanded analogs of 2-ethoxyestradiol resemble paclitaxel in their ability to enhance tubulin polymerization and stabilize microtubules (Wang et al., 2000). We have therefore synthesized a variety of additional B-ring homologated analogs of 2-ethoxyestradiol, including the benzo[*f*]azepine derivative **32** (Scheme 2). Treatment of 2-ethoxy-3,17 β -diacetoxy-6-oxoestra-1,3,5(10)-triene (**43**) (Cushman et al., 1997) with hydroxylamine resulted in selective deacetylation of the phenolic acetate as well as oxime formation to afford **8**. There are several reports of the use of oxime tosylates as substrates for Beckmann rearrangements (Tamura et al., 1973; Ciattini et al., 1990). These rearrangements are reported to occur when the oxime tosylate is passed through a column of acidic or basic alumina. Reaction of **8** with tosyl chloride in pyridine resulted in the formation

of the oxime tosylate, which underwent the desired Beckmann rearrangement when passed through a column of basic alumina and eluted with a mixture of benzene and chloroform to afford the lactam **44**. Diborane reduction of **44** yielded the expected benzo[*f*]azepine system **45**. Reaction of **45** with acetic anhydride resulted in acetylation of both alcohols as well as the amine to give **46**, which was hydrolyzed with sodium hydroxide to provide the diol **47**. Diborane reduction of the amide present in **47** produced the desired product **32**.

Oxidation of the B ring of 2-ethoxyestradiol has afforded a number of very potent cytotoxic tubulin polymerization inhibitors (Cushman et al., 1997). These included 2-ethoxy-6-oxoestradiol and the corresponding oxime. Methods have therefore been sought for oxidation of the B ring of 2-ethoxyestradiol. As shown in Scheme 3, treatment of 2-ethoxy-6-oxoestradiol diacetate (**43**) (Cushman et al., 1997) with triflic anhydride under basic conditions afforded the enol triflate **48**, which was reduced in the presence of formic acid, triethylamine, triphenylphosphine, and palladium acetate in DMF to afford the cyclic alkene **33** (Ciattini et al., 1990). Instead of the expected 6 α ,7 α -epoxide, oxidation of **33** with *m*-chloroperbenzoic acid gave compounds **49** and **50**, which are the addition products of *m*-chloroperbenzoic acid to the 6 α ,7 α -epoxide (Burdett et al., 1982). The stereochemical assignments are based on the larger axial-equatorial coupling observed between the C-6 and C-7 methine protons in **49** ($J = 3.5$ Hz) versus the smaller diequatorial coupling constant ($J = 2.2$ Hz) seen with **50** (Jackman and Sternhell, 1969). Lithium aluminum hydride reduction of **49** and **50** cleaved all of the esters, resulting in the tetraols **51** and **7**. Oxidation of the starting material **43** with chromium trioxide in acetic acid gave the α -hydroxyketone **6**.

2-MEO Effects on DNA Synthesis, Proliferation and Cell-Cycle Distribution of Human Airway Smooth Muscle Cells

2-MEO (0.3–10 μ M) concentration-dependently inhibited 3 H-thymidine incorporation in cultures of human airway smooth muscle cells (Table 1). Cell enumeration experiments revealed that 2-MEO (10 μ M) prevented 0.3 U/ml thrombin-induced increase in cell number but had no effect on the number of nonviable cells after incubation for 48 h (Table 2). Flow cytometric analyses of cell-cycle distribution (Fig. 1) indicated that 2-MEO (10 μ M) reduced the proportion of cells in S-phase and increased that in G₂/M (Table 3). In a separate series of experiments, the incubation of cells with thrombin (0.3 U/ml) increased cell number ($\times 10^{-4}$ well of a 6-well plate) from 29.8 ± 3.9 to 45.5 ± 8.5 ; this was significantly reduced ($P < 0.05$, paired *t* test) to 33.8 ± 6.7 and 32.0 ± 5.0 , for 2-MEO (10 μ M) and compound **5**, respectively, without concomitant increase in the number of trypan blue staining (i.e., nonviable) cells.

Inhibition of Human Airway Smooth Muscle DNA Synthesis by 2-MEO Analogs

The range of data obtained for DNA synthesis inhibition in cultures of human airway smooth muscle (Tables 4–6) was narrow, covering only one order of magnitude for active compounds. The most potent inhibitors were the 2-ethoxyestradiol derivatives **8** and **6**, 2-(hydroximino)estradiol (**13**) and ICI 182,780 (**17**) (pIC_{50} for DNA synthesis inhibition of 5.99, 5.97, 5.95, and 5.88, respectively), all being considerably

more potent than 2-MEO itself (pIC_{50} 5.21). Compound **6** also displays negligible ER binding potency (see below). Both **8** and **6** are acetylated at the 17 position (R5), although this feature is itself not sufficient for potent DNA synthesis inhibition, because other acetylated compounds show reduced activity (e.g., the diacetylated **33**, pIC_{50} 5.24). Two compounds, **3** and **36**, stimulated rather than inhibited DNA synthesis; these compounds were not examined further by CoMFA.

Displacement of [³H]Estradiol from Rat Uterine ER

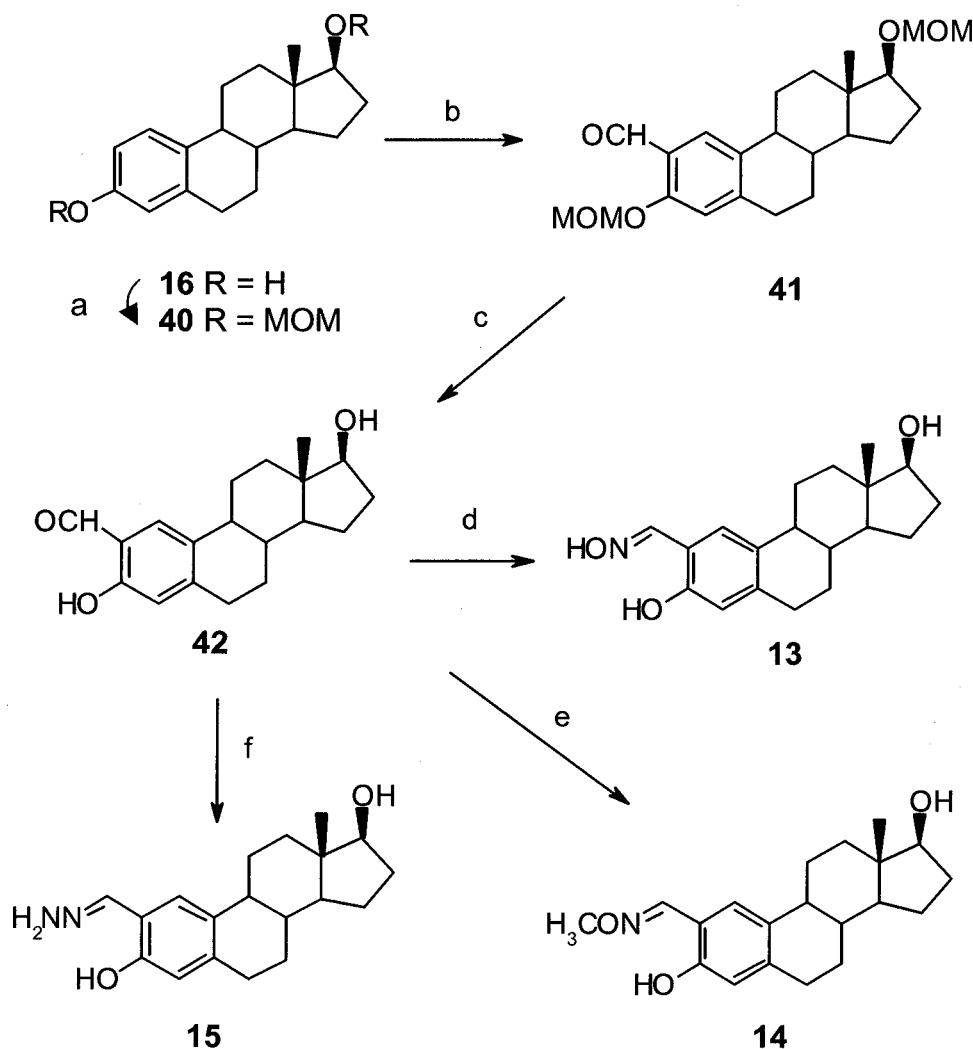
In contrast to the data obtained for DNA synthesis inhibition, ER binding affinities covered a much larger range of values (approximately 5 orders of magnitude; Tables 4–6). The most potent displacement activity was exhibited by **16**, **34**, and **19** (pIC_{50} for ER binding of 9.89, 9.77, and 9.49, respectively). All compounds tested with a seven-membered B ring (Table 2) were devoid of ER binding, although most of these analogs retained DNA synthesis inhibition (**23–31**). Some compounds tested were potent inhibitors of DNA synthesis and ER binding (e.g., **13**, pIC_{50} for DNA synthesis inhibition of 5.95, pIC_{50} for ER binding 9.16). Overall, however, there was no correlation between potency in the two

biological assays ($r^2 = 0.038$ for the 23 compounds for which biological potency was determined in both assays).

Generation and Optimization of 3D-QSARs

Selection of Optimal Alignments. Table 7 shows the q^2 obtained for the preliminary CoMFA models obtained from the four different alignments for DNA synthesis inhibition and ER binding data. For DNA synthesis inhibition data, the q^2 values obtained were low, indicative of models of limited predictive values. Using the default cut-off (30 kcal/mol^{-1}), alignment 4 gave the most predictive model ($q^2 = 0.144$); this alignment was thus used to generate optimized models. For ER binding, the highest q^2 values were obtained for alignments 1 and 3 ($q^2 = 0.776$ and 0.760 , respectively). Optimized CoMFA plots were subsequently generated from alignment 3, because initial CoMFA plots obtained from alignment 1 were poorly defined, and difficult to interpret, even after preliminary attempts to optimize them (data not shown).

Optimization of CoMFA Models. Optimized CoMFA models were obtained from the preliminary models by systematically altering user-modifiable parameters—cut-off energy, field-strength scaling, and dropping electrostatic values



Scheme 1. Reagents and conditions: a, $\text{CH}_3\text{OCH}_2\text{Cl}$, $i\text{-Pr}_2\text{EtN}$, THF, 60°C (8 h); b, (1) sec-BuLi , THF, -78°C (2.5 h), (2) DMF, -78 to 23°C (3 h); c, LiBF_4 , aq CH_3CN , 72°C (5 h); d, $\text{H}_2\text{NOH}\cdot\text{HCl}$, pyridine, 90°C (1 h); e, H_2NOCH_3 , pyridine, 90°C (2 h); f, $\text{H}_2\text{NNH}_2\cdot 2\text{HCl}$, pyridine, 90°C (2 h).

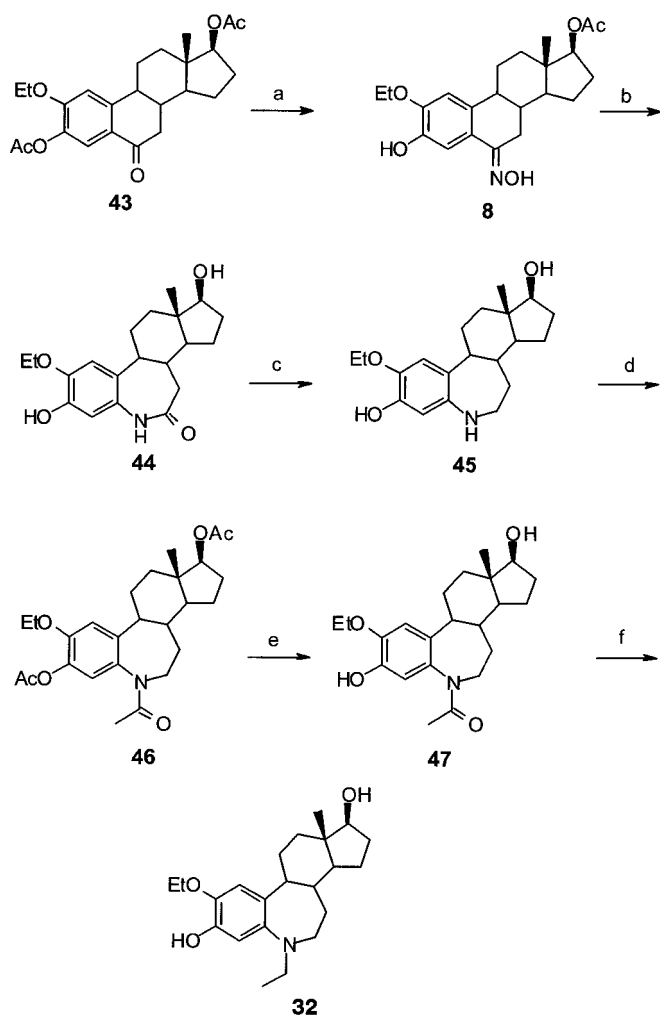
at the steric maximum—and examining the effects of removing outliers. For DNA synthesis inhibition, parameter optimization alone gave a model with improved predictivity ($q^2 = 0.377$, see Table 8). Examination of this model revealed one compound (the hydroximino derivative **13**) for which the residual was greater than three times the S.E.M. residual. Elimination of this compound from the data set and reoptimization with respect to user-modifiable parameters further improved the model ($q^2 = 0.483$). No additional outliers could be detected on the basis of compound residuals. We therefore chose to rederive the model in the absence of each compound in turn. The greatest increase in q^2 ($q^2 = 0.566$) was obtained when the 7α -substituted compound, ICI 182,780 (**17**), was removed. The model thus obtained could not be further optimized by changing the user-modifiable parameters. A summary of the optimization process for the DNA synthesis CoMFA model can be found in Table 8.

For ER binding, systematic alterations to user-modifiable parameters produced only a modest change in predictivity ($q^2 = 0.773$). One compound (the parent compound **1**) could be classified as an outlier with regard to its residual (residual 0.375, compared with the S.D. of the residuals for the dataset

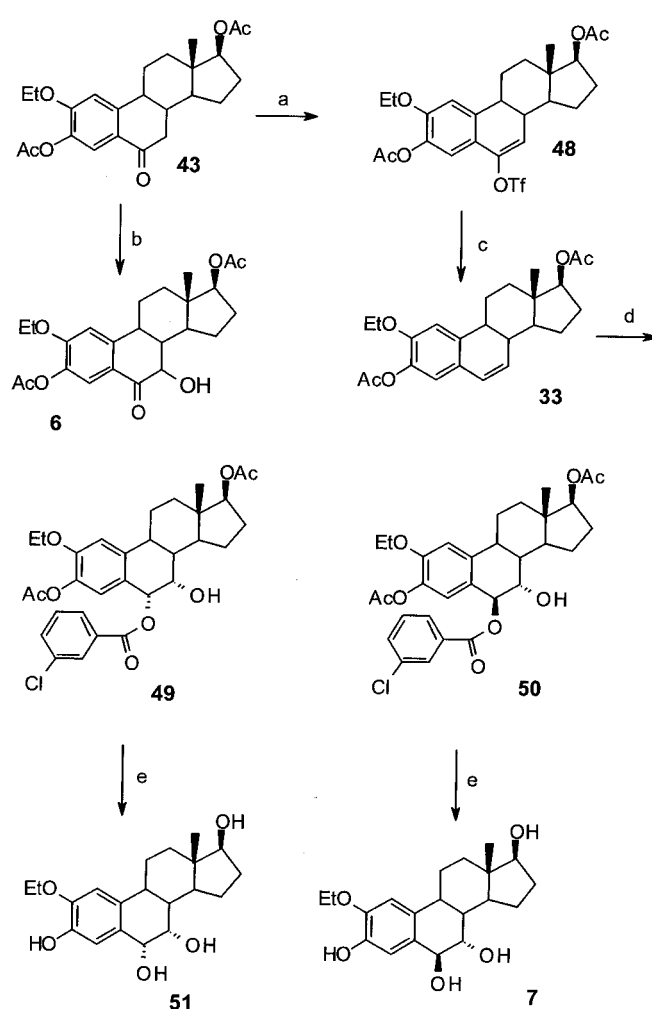
of 0.114). However, re-derivation of a model without this compound gave only a minor change in q^2 (0.799). Thus, compound **1** was not omitted.

Final CoMFA Models. The features of the final CoMFA models—one for DNA synthesis inhibition, one for ER binding—are described in Table 9. Apart from differences described above in the parameters used to derive them (alignment, use of scaling, cut-offs, etc.), the two models show other distinct quantitative differences: the CoMFA model for DNA synthesis inhibition has less predictive power than that obtained for ER binding (q^2 of 0.566 versus q^2 of 0.773); the model for DNA synthesis (three components) is simpler than that for ER binding (eight components); and the relative contributions to the models from steric and electrostatic descriptors is reversed in the two models (72% steric and 28% electrostatic contribution for DNA synthesis contribution versus 32% steric and 68% electrostatic for ER binding).

Qualitative differences between the two CoMFA models can be observed in electrostatic and steric CoMFA contour plots (Figs. 2 and 3). For DNA synthesis inhibition, favorable electrostatic regions are limited (Fig. 2, a and c): blue polyhedra, signifying regions where electropositive substitutions



Scheme 2. Reagents and conditions: a, $H_2NOH \cdot HCl$, pyridine, $100^\circ C$ (30 min); b, (1) $TsCl$, pyridine, $23^\circ C$ (2 h), (2) Al_2O_3 , $CHCl_3-C_6H_6$; c, B_2H_6 , THF, $23^\circ C$ (6 h) and reflux (4 h); d, Ac_2O , pyridine, $23^\circ C$ (12 h); e, $Aq NaOH$, $MeOH$, $23^\circ C$ (4.5 h); f, B_2H_6 , THF, $23^\circ C$ (4 h) and reflux (4 h).



Scheme 3. Reagents and conditions: a, $(TfO)_2O$, 2,6-(*t*-Bu)-4-Me-pyridine, CH_2Cl_2 , $0^\circ C$ (3 h); b, CrO_3 , $AcOH$, $12-15^\circ C$ (3 h); c, $HCOOH$, Et_3N , Ph_3P , $Pd(Ac)_2$, DMF , 60 to $62^\circ C$ (3 h); d, $MCPBA$, $TsOH$, CH_2Cl_2 , $23^\circ C$ (20 h); e, $LiAlH_4$, THF, reflux (14 h).

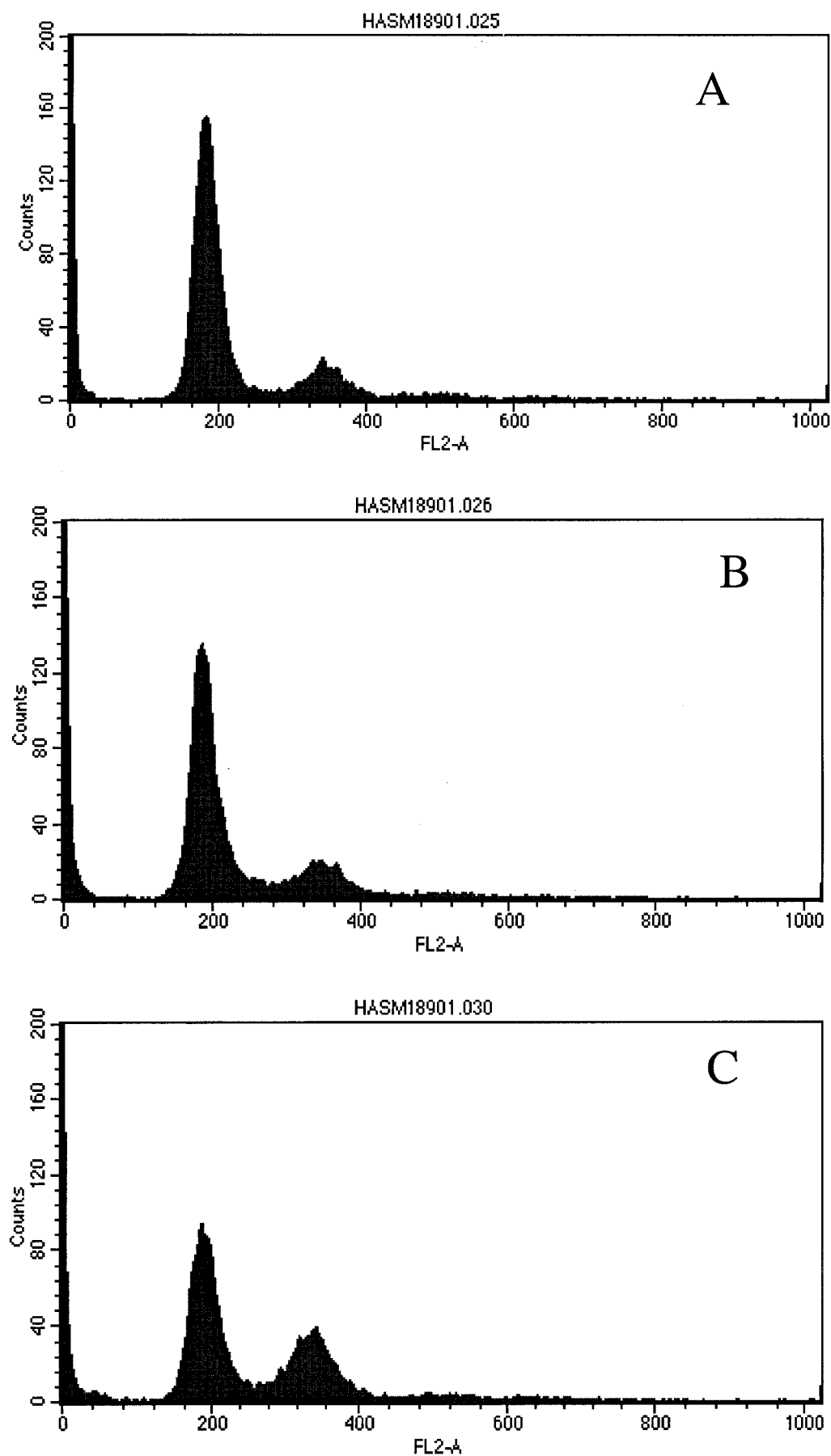


Fig. 1. Influence of thrombin (0.3 U/ml) on propidium iodide DNA profiles in human airway smooth muscle cells in culture and its modification by 2-MEO (10 μ M). These profiles are representative of 12 others (see Table 2) and show that thrombin (B) increases the proportion of cells in S-phase over that observed in unstimulated cells (A). The thrombin-induced increase in cells in S-phase is prevented by 2-MEO (C), which also increases the proportion of cells in G₂/M.

favor biological activity, can be found in the 2 position of the steroid nucleus below the plane of the A ring, and in the vicinity of the 17 β substitutions. An additional small red polyhedron (favorable position for electronegative substitution) can be seen near the B ring. In direct contrast, ER binding is favored by electronegative properties near the A ring, as evidenced by several red polyhedra situated above and below the plane of the A ring. (Fig. 2, b and d). The blue polyhedron near the 17 β position suggests that electropositive substitutions in this region also favor ER binding, as is the case for DNA synthesis inhibition.

The steric CoMFA field for DNA synthesis inhibition (Fig. 3, a and c) defines three regions in which increased steric bulk favors activity (green polyhedra): in the plane of the A ring near the 2-position; in the plane of the B ring; and an area near the 17 position, roughly in the plane of the D ring. The steric contributions are further defined by areas in which steric bulk is not favorable to DNA synthesis inhibition activity (yellow polyhedra), with the major regions above and below the planes of both the A ring (near the 2 position) and the B ring. The steric field for ER binding is, in comparison, less well defined. The main constraints on steric bulk are found in the vicinity of the 2 position—a positive steric influence on activity (green polyhedron, located in the plane of the A ring), and a nearby region of negative steric influence (yellow polyhedron, below the plane of the A ring; Fig. 3, b and d). Although the most potent compound for ER binding, estradiol (**16**), has no substituent in this position, several other compounds that do display good ER binding (e.g., **11** and **13**) are 2-substituted; presumably, these latter compounds give rise to the positive correlation between bulk in this position and ER binding. An additional region in which steric bulk positively correlates with improved ER binding can be found near the 17 position.

Discussion

Antitumor and anti-inflammatory therapeutic regimens are often optimized by the combination of two or more agents having complementary actions on different aspects of these complex pathologies. In particular, the recent description by members of Folkman's laboratory of synergy between antiproliferative cytotoxic agents and agents that specifically target angiogenesis (Nguyen et al., 1994) pro-

TABLE 7
q² values for preliminary CoMFA models for DNA synthesis inhibition (DNA q²) and ER binding (ER q²) for the four different alignments

	Alignment			
	1	2	3	4
DNA q ²	0.011	-0.062	0.127	0.144
ER q ²	0.776	0.624	0.760	0.636

TABLE 8
q² values obtained for CoMFA models obtained for DNA synthesis inhibition after removal of statistically outlying compounds and reoptimization of the CoMFA model

	Outlier Optimization Run		
	1	2	3
Compound Excluded		13	13,17
q ²	0.377	0.483	0.566

vides direct evidence of the synergistic nature of combining these two activities in reducing tumor growth. In contrast, antagonists of single receptor classes used alone are rarely clinically useful in the treatment of chronic inflammatory conditions. Moreover, tumor chemotherapy regimens exploit synergies to achieve maximal tumor shrinkage. 2-Methoxyestradiol (**1**) is an attractive lead compound for the development of novel therapeutic agents to treat these diseases, because its structure provides for multiple individual activities that may sum or even amplify to provide an effective anti-inflammatory and antitumor agent. These activities include the inhibition of cell cycle progression through DNA synthesis inhibition (G₁ arrest; Stewart et al., 1999b) and microtubule dysfunction (G₂/M arrest; D'Amato et al., 1994; Fotsis et al., 1994; Cushman et al., 1995; Hamel et al., 1996), in addition to antiangiogenic actions via a direct inhibitory effect on endothelial cells (Klauber et al., 1997; Reiser et al., 1998; Tsukamoto et al., 1998). In contrast, with the possible exception of estrogen-responsive tumors, it is unlikely that affinity for ER would enhance the potential beneficial actions of 2-MEO. In the present study, we have developed 3D-QSAR models based on 2-MEO and a series of analogs that may guide the development of novel molecules that possess more or less potency as appropriate for the attributes that seem to be of potential therapeutic relevance.

Inhibition of [³H]thymidine uptake into the airways smooth muscle cells by 2-MEO and analogs has a number of potential interpretations including: direct reduction of the activity of enzymes responsible for DNA synthesis; induction of cell cytotoxicity; influence on the transport of thymidine into the cell; arrest of mitogen-stimulated cells in G₀/G₁ of the cell-cycle. In the case of 2-MEO, which is likely to have activity indicative of its analogs, there was no evidence of cytotoxicity (loss of membrane integrity or apoptosis or a reduction in cell number under basal conditions) at the maximum concentration used (10 μ M). The reduction in thymidine uptake was paralleled by a reduction in cells entering S-phase, arguing against the former observation being explained by direct inhibition of thymidine transport. The reduction in indices of S-phase entry was accompanied by a reduction in thrombin-induced increases in cell number, indicating an antiproliferative ef-

TABLE 9
Summary of final CoMFA models for DNA synthesis inhibition and ER binding.

Parameter	CoMFA Model	
	DNA Synthesis Inhibition	ER Binding
Alignment Used	#4	#3
Number of Compounds	35	25
Outliers Omitted	13, 17	None
Steric/Electrostatic Cut-Off	100 kcal/mol	80 kcal/mol
Scaling	None	CoMFA Standard
Electrostatics Dropped	No	Yes
q ²	0.566	0.773
Number of Components	3	8
r ²	0.866	0.997
S.E.	0.107	0.125
Steric Contribution to Molecular Field	0.719	0.317
Electrostatic Contribution to Molecular Field	0.281	0.683

fect. Time course studies indicate that when 2-MEO is added more than 6 h after thrombin, there is no inhibition of [^3H]thymidine incorporation (measured at 24–28 h after thrombin addition; T. Harris and A. G. Stewart, unpublished observations), in contrast to the expected rapid onset of action if 2-MEO were acting by direct inhibition of DNA synthesis enzymes. Thus, the effect on [^3H]thymidine incorporation of 2-MEO, and most probably that of its analogs, is explained by arrest of cells in G_0/G_1 phase of the cell cycle leading to an antiproliferative effect that is contributed to by a further action, identified by fluorescence-activated cell-sorting studies, to arrest cells in G_2/M phase of the cell-cycle.

The QSAR models were generated using the CoMFA method, developed by Cramer et al. (1988). CoMFA models are known to be sensitive both to the alignment of the molecules (indicative of the orientation of the molecules when they bind to their receptor) as well as to the conformation of the individual molecules in the alignment (the conformation they adopt when binding). In the absence of definitive knowledge of these modes of binding of the compounds, one must examine several alignments and conformations and select the combination that gives the CoMFA model with the greatest predictive power (i.e., the highest q^2). In this study, optimal models for DNA synthesis inhibition and ER binding were obtained from different align-

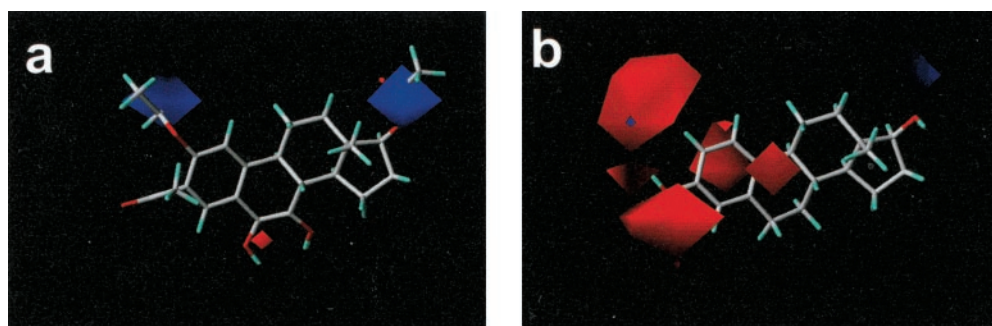


Fig. 2. Orthogonal views of CoMFA contour plots of electrostatic field contributions to DNA synthesis inhibition (a and c) and ER binding (b and d). A potent compound in each of the two assays is depicted: compound **6** for DNA synthesis inhibition; estradiol (**16**) for ER binding. Blue polyhedra correspond to regions in which biological activity is favored by increased positive charge, whereas red polyhedra define regions in which more negative charge is favorable to biological activity.

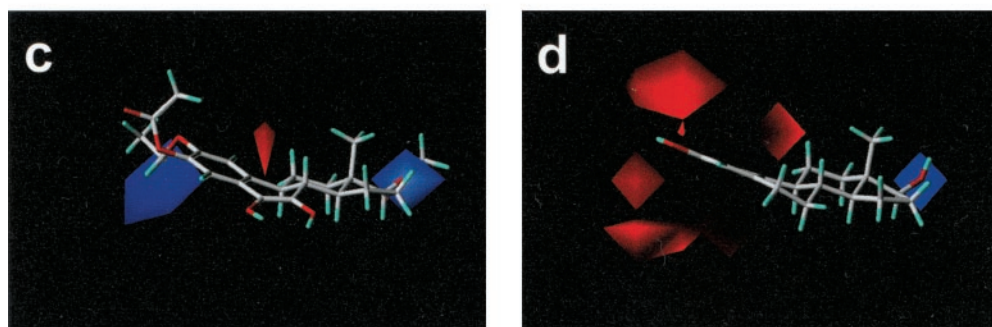


Fig. 3. Orthogonal views of CoMFA contour plots of steric field contributions to DNA synthesis inhibition (a and c) and ER binding (b and d). A potent compound in each of the two assays is depicted: compound **6** for DNA synthesis inhibition; estradiol (**16**) for ER binding. Green polyhedra correspond to regions in which biological activity is favored by increased steric bulk, whereas yellow polyhedra define regions in which reduced steric bulk is favorable to biological activity.

ments. For DNA synthesis inhibition, the best alignment was found to occur when the conformation of the substituents in the 2 and 3 positions (R1 and R2) was adjusted to match the conformation of the corresponding substituents in 2-MEO (methoxy- and hydroxy-). Conversely, a better preliminary CoMFA model derived for ER binding was obtained when these substituents were not constrained to 2-MEO-like conformation, but rather set to the lowest energy positions. Differences were also observed in the choice of CoMFA parameters giving the best models as well as in the relative contributions to these models of the steric and electrostatic fields (Table 9). Together, these data suggest that the receptor for DNA synthesis inhibition requires quite different conformational and structural features of its ligands compared with those required by the ER.

The design of compounds more potent in inhibiting DNA synthesis can be assisted by the identification of structural features important for this biological activity. The CoMFA studies described here offer a means to discover these features. The two most potent compounds for DNA synthesis inhibition (**8** and **6**) both have ethoxy substituents at R1 and are acetylated at R5. These structural features are reflected in the steric CoMFA field for DNA synthesis inhibition, which shows favorable regions for steric bulk in the region of both R1 and R5 (Fig. 3, a and c). The electrostatic CoMFA field for DNA synthesis inhibition indicates a preference for relatively electropositive substituents in these positions. At R1, this is probably a consequence of weakly active or inactive compounds bearing substituents with electronegative atoms (e.g., the formyl substituent of **9** and **10**; the hydrazone group of **15**). At R5, this region is centered on the carbonyl carbon atom found in acetylated compounds with good DNA synthesis inhibitory potency (e.g., **8**, **6**, **21**, and **26**). The additional favorable region for steric bulk and negative charge near R3 probably arises exclusively from the high biological activity exhibited by **8** (R3 = hydroximino), **6** (R3 = hydroxyl/keto), and **5** (R3 = keto). Several compounds with large substituents in the R2 region (e.g., the benzyl derivatives **2**, **10**, **18**, and **26**) are inactive; consequently, sterically disfavored regions appear in the CoMFA contour plots in the region of the A ring. It has been shown previously that size constraints on A ring substituents for another biological activity of 2-MEO derivatives, where short, unbranched sidechains have been shown to favor inhibition of tubulin polymerization (Cushman et al., 1995). The relationship between antiproliferative activity and microtubule assembly has been questioned by data from Attalla et al. (1996) who suggest that the action of 2-MEO is caused by a paclitaxel-like effect on tubulin dynamics inducing a functional defect in the mitotic spindle. Novel 2-MEO analogs substituted to achieve a paclitaxel-like structure have increased potency as agents that enhance tubulin polymerization without appreciable affinity for the colchicine binding site on tubulin (Verdier-Pinard et al., 2000) and are potent antiproliferative agents [e.g., 2-ethoxyestradiol-17 β -acetate (Cushman et al., 1997)]. Whether the similarity between the current QSAR model and the SAR observations on cytotoxicity (Cushman et al., 1997) reflects a similar mechanism of action for cytotoxicity and DNA synthesis inhibition remains unclear. Other inhibitors of microtubule function either increase (e.g., colchicine) or decrease (e.g., paclitaxel)

airway smooth muscle DNA synthesis (T. Harris and A. G. Stewart, unpublished observations), which is not inconsistent with the inhibition of DNA synthesis by the analogs used to generate the QSAR being related to a paclitaxel-like effect.

In this study, we have identified compounds with reasonable potency for inhibition of DNA synthesis but that show relatively little ER affinity (e.g., **6** and **5**). A similar separation of ER affinity and antitubulin action with analogs of 2-MEO has been noted (Cushman et al., 1997). Nevertheless, airway smooth muscle cells in culture express high affinity ER binding sites ($K_D = 0.53$ nM; see *Methods*) and antibodies detecting both ER α and ER β revealed immunoreactive ER in the cytoplasm and more prominently in the nucleus of cultured airway smooth muscle (T. Harris and A. G. Stewart, unpublished observations). The rat uterine cytosol used to generate the ER affinity data for the QSAR is known to contain predominantly ER α . It seems unlikely that the compounds used to generate the QSAR would bind to ER β with markedly different affinities to ER α as previous binding studies show that some of the compounds used in the present study (compounds **16**, **19**, **34**, and **37**) have affinities not more than 3-fold different between the two receptor isoforms (Kuiper et al., 1997) and it has recently been reported that 2-MEO has a lower affinity for ER β than ER α (Pribluda et al., 2001). These observations are not consistent with a specific role for ER β in the effects of 2-MEO analogs.

The lack of correlation between DNA synthesis inhibition and ER binding, as well as the differences between the CoMFA models for the two activities suggest that compounds even more selective for DNA synthesis inhibition could be designed. For example, the electrostatic CoMFA field for ER binding shows multiple electronegative-favoring regions above and below the plane of the A ring, which are not present in the model for DNA synthesis inhibition. These regions resemble the electrostatic CoMFA field obtained in an earlier study of the mitogenic effects of estradiol analogs (Wiese et al., 1997), despite the fact that the two studies were derived from different data sets. This similarity of models across structurally diverse molecules suggests that the requirements for ER binding are relatively stringent. This latter hypothesis is consistent with the fact that the data sets include compounds that fit ER well (i.e., they have high affinity). Indeed, estrogen has been shown to bind snugly at a site near the region of the monomer of ER α that is involved with dimerization, as determined by X-ray crystallographic studies (Tanenbaum et al., 1998). In our explorations for analogs of 2-MEO with increased potency for DNA synthesis inhibition, we will attempt to design molecules lacking ER affinity, using the knowledge of these stringent requirements for ER binding.

Derivation of CoMFA models for DNA synthesis inhibition from a complete data set (37 compounds) gave models with poor predictive capability, as assessed by the low values obtained for q^2 derived from cross-validated analyses. Models with significantly greater predictive power could be obtained by excluding outliers, identified in an iterative manner. Although the act of excluding outliers is inherently unsatisfying, it is accepted practice in QSAR studies to omit such compounds in the spirit of developing

more predictive models (Raghavan et al., 1995). Of the two compounds excluded, ICI 182,780 (**17**) is unique in the data set, in that it possesses a long and potentially flexible side chain at R4. It is easy to see in hindsight that the conformation of this side chain would be difficult to model. A structural rationale for the outlying behavior of the other outlier **13** is more difficult to find. It is the third most potent compound tested in the data set but is the only compound with an aromatic hydroximino substituent. It may be that the conjugated nature of this group renders its electronic properties difficult to model (e.g., with respect to its hydrogen bonding characteristics). The inclusion of other analogs with similar (e.g., hydroxyalkyl) substituents in this region might be required to yield predictive models that include compound **13**.

In summary, we have developed a CoMFA model for DNA synthesis inhibition in airway smooth muscle for a set of analogs of 2-MEO. The model differs in a number of characteristics from models derived for ER binding from a related data set. Application of this molecular modeling approach to the microtubule action of 2-MEO and analogs may also be valuable, because it seems likely that microtubule dysfunction would result in dose- and indication-limiting cytotoxic side effects, such as those seen with colchicine and paclitaxel. These models would be valuable tools to assist in the design of compounds with improved potency with regards to DNA synthesis inhibition, while minimizing undesired effects through ER binding and effects on microtubule function.

Acknowledgments

We thank John Wilson and the staff of the Respiratory Medicine and Pathology Departments at the Alfred Hospital, Prahran, for providing specimens of human airway tissue.

References

- Andrews PR, Craik DJ, and Martin JL (1984) Functional group contributions to drug-receptor interactions. *J Med Chem* **27**:1648–1657.
- Arnsperger GM, Carlson KE, and Katzenellenbogen JA (1997) The estradiol pharmacophore: ligand structure-estrogen receptor binding affinity relationships and a model for the receptor binding site. *Steroids* **62**:268–303.
- Arbiser JL, Panigrahy D, Klauber N, Rupnick M, Flynn E, Udagawa T, and D'Amato RJ (1999) The antiangiogenic agents TNP-470 and 2-methoxyestradiol inhibit the growth of angiosarcoma in mice. *J Am Acad Dermatol* **40**:925–929.
- Attala H, Makela TP, Adlercreutz H, and Andersson LC (1996) 2-Methoxyestradiol arrests cells in mitosis without depolymerizing tubulin. *Biochem Biophys Res Commun* **228**:467–473.
- Brouchet L, Krust A, Dupont S, Chambon P, Bayard F, and Arnal JF (2001) Estradiol accelerates reendothelialization in mouse carotid artery through estrogen receptor- α but not estrogen receptor- β . *Circulation* **103**:423–428.
- Burdett J, Rao P, Kim H, Hyun K, Karten M, and Blye R (1982) Synthesis of 17 α -ethynyl-7 α ,11 β -dihydroxyestra-1,3,5(10)-triene-3,17 β -diol. *J Chem Soc Perkin Trans* **1982**:2877–2880.
- Ciattini M, Enrico M, and Giorgio O (1990) An efficient preparation of 6,7-didehydroestrogens. *Synth Commun* **1990**:1293–1297.
- Cramer RD III, Patterson DE, and Bunce JD (1988) Comparative molecular field analysis (CoMFA). 1. Effect of shape on binding of steroids to carrier proteins. *J Am Chem Soc* **110**:5959–5967.
- Cushman M, He H-M, Katzenellenbogen JA, Lin CM, and Hamel E (1995) Synthesis, antitubulin and antimetabolic activity, and cytotoxicity of analogs of 2-methoxyestradiol, an endogenous mammalian metabolite of estradiol that inhibits tubulin polymerization by binding to the colchicine binding site. *J Med Chem* **38**:2041–2049.
- Cushman M, He H-M, Katzenellenbogen JA, Varma RK, Hamel E, Lin CM, Ram S, and Sachdeva YP (1997) Synthesis of analogs of 2-methoxyestradiol with enhanced inhibitory effects on tubulin polymerization and cancer cell growth. *J Med Chem* **40**:2323–2334.
- D'Amato RJ, Lin CM, Flynn E, Folkman J, and Hamel E (1994) 2-Methoxyestradiol, an endogenous mammalian metabolite, inhibits tubulin polymerization by interacting at the colchicine site. *Proc Natl Acad Sci USA* **91**:3964–3968.
- Eriksson HA, Hardin JW, Markaverich B, Upchurch S, and Clark JH (1980) Estrogen binding in the rat uterus: heterogeneity of sites and relation to uterotrophic response. *J Steroid Biochem* **12**:121–130.
- Fernandes D, Guida E, Koutsoubos V, Harris T, Vadiveloo PK, Wilson J, and Stewart AG (1999) Glucocorticoids inhibit proliferation, cyclin D1 expression and retinoblastoma protein phosphorylation, but not activity of the extracellular regulated kinases (ERK) in human cultured airway smooth muscle. *Am J Respir Cell Mol Biol* **21**:77–88.
- Fotsis T, Zhang Y, Pepper MS, Adlercreutz H, Montesano R, Nawroth PP, and Schweigerer L (1994) The endogenous oestrogen metabolite 2-methoxyestradiol inhibits angiogenesis and suppresses tumour growth. *Nature (Lond)* **368**:237–239.
- Gasteiger J and Marsili M (1980) Iterative partial equalization of orbital electro-negativity—a rapid access to atomic charges. *Tetrahedron* **36**:3219–3228.
- Hamel E, Lin CM, Flynn E, and D'Amato RJ (1996) Interactions of 2-methoxyestradiol, an endogenous mammalian metabolite, with unpolymerized tubulin and with tubulin polymers. *Biochemistry* **35**:1304–1310.
- Hodgin JB, Kregel JH, Reddick RL, Korach KS, Smithies O, and Maeda N (2001) Estrogen receptor α is a major mediator of 17 β -estradiol's atheroprotective effects on lesion size in ApoE $-/-$ mice. *J Clin Invest* **107**:333–340.
- Ireland R and Varney M (1986) Approach to the total synthesis of chlorothricolide: synthesis of (\pm)-19,20-dihydro-24-O-methylchlorothricolide, methyl ester, ethyl carbonate. *J Org Chem* **51**:635–648.
- Jackman LM and Sternhell S (1969) *Applications of Nuclear Magnetic Resonance Spectroscopy in Organic Chemistry*. 2nd ed, Pergamon Press, Oxford.
- Josefsson E and Tarkowski A (1997) Suppression of type II collagen-induced arthritis by the endogenous estrogen metabolite 2-methoxyestradiol. *Arthritis Rheum* **40**:154–163.
- Klauber N, Parangi S, Flynn E, Hamel E, and D'Amato RJ (1997) Inhibition of angiogenesis and breast cancer in mice by the microtubule inhibitors 2-methoxyestradiol and Taxol. *Cancer Res* **57**:81–86.
- Kuiper GG, Carlsson B, Grandien K, Enmark E, Haggblad J, Nilsson S, and Gustafsson JA (1997) Comparison of the ligand binding specificity and transcript tissue distribution of estrogen receptors α and β . *Endocrinology* **138**:863–870.
- Lottering M-L, Haag M, and Seegers JC (1992) Effects of 17 β -estradiol metabolites on cell cycle events in MCF-7 cells. *Cancer Res* **52**:5926–5932.
- Markaverich BM and Clark JH (1979) Two binding sites for estradiol in rat uterine nuclei: relationship to uterotrophic response. *Endocrinology* **105**:1458–1462.
- Nguyen M, Watanabe H, Budson AE, Richie JP, Hayes DF, and Folkman J (1994) Elevated levels of an angiogenic peptide, basic fibroblast growth factor, in the urine of patients with a wide spectrum of cancers. *J Natl Cancer Inst* **86**:356–361.
- Nishigaki I, Sasaguri Y, and Yagi K (1995) Anti-proliferative effect of 2-methoxyestradiol on cultured smooth muscle cells from rabbit aorta. *Atherosclerosis* **113**:167–170.
- Pribluda VS, LaVallee TM, and Green SJ (2001) 2-Methoxyestradiol A novel endogenous chemotherapeutic agent, in *The New Angiotherapy* (Fan TP and Kohn EC eds) pp 387–407, Humana Press, Totowa, NJ.
- Raghavan K, Buolamwini JK, Fesen MR, Pommier Y, Kohn KW, and Weinstein JN (1995) Three-dimensional quantitative structure-activity relationship (QSAR) of HIV integrase inhibitors: a comparative molecular field analysis (CoMFA) study. *J Med Chem* **38**:890–897.
- Reiser F, Way D, Bernas M, Witte M, and Witte C (1998) Inhibition of normal and experimental angiotumor endothelial cell proliferation and cell cycle progression by 2-methoxyestradiol. *Proc Soc Exp Biol Med* **219**:211–216.
- Sadler BR, Cho SJ, Ishaq KS, Chae K, and Korach KS (1998) Three-dimensional quantitative structure-activity relationship study of nonsteroidal estrogen receptor ligands using the comparative molecular field analysis/cross-validated r²-guided region selection approach. *J Med Chem* **41**:2261–2267.
- Schumacher G, Kataoka M, Roth JA, and Mukhopadhyay T (1999) Potent antitumor activity of 2-methoxyestradiol in human pancreatic cancer cell lines. *Clin Cancer Res* **5**:493–499.
- Stewart AG, Harris T, Fernandes DJ, Schachte LC, Koutsoubos V, Guida E, Ravenhall CE, Vadiveloo P, and Wilson JW (1999a) β_2 -Adrenergic receptor agonists and cAMP arrest human cultured airway smooth muscle cells in the G₁ phase of the cell cycle: role of proteasome degradation of cyclin D1. *Mol Pharmacol* **56**:1079–1086.
- Stewart AG, Harris T, Guida E, Vlahos R, Koutsoubos V, Hughes R, and Robertson A (1999b) The estradiol metabolite, 2-methoxyestradiol inhibits proliferation of human cultured airway smooth muscle. *Am J Crit Care Med* **159**:A531.
- Stewart AG, Vlahos R, Fernandes DJ, and Hughes RA (2001) Oestradiol Metabolites effects on airway wall remodelling, in *Progress in Respiration Research* (Hansel TT and Barnes PJ eds) vol 31, pp 102–105, Karger, Basel, Switzerland.
- Tamura Y, Sumoto K, Fujii S, Satoh H, and Ikeda M (1973) Diethoxyacetalization with *O*-mesitylenesulfonylhydroxylamine. *Synthesis* **1973**:312.
- Tanenbaum DM, Wang Y, Williams SP, and Sigler PB (1998) Crystallographic comparison of the estrogen and progesterone receptor's ligand binding domains. *Proc Natl Acad Sci USA* **95**:5998–6003.
- Tsakamoto A, Kaneko Y, Yoshida T, Han K, Ichinose M, and Kimura S (1998) 2-Methoxyestradiol, an endogenous metabolite of estrogen, enhances apoptosis and β -galactosidase expression in vascular endothelial cells. *Biochem Biophys Res Commun* **248**:9–12.
- Verdier-Pinard P, Wang Z, Mohanakrishnan AK, Cushman M, and Hamel E (2000) A steroid derivative with paclitaxel-like effects on tubulin polymerization. *Mol Pharmacol* **57**:568–575.
- Wang Z, Yang D, Mohanakrishnan AK, Fanwick PE, Nampoothiri P, Hamel E, and Cushman M (2000) Synthesis of B-ring homologated estradiol analogues that

- modulate tubulin polymerization and microtubule stability. *J Med Chem* **43**:2419–2429.
- Wiese TE, Polin LA, Palomino E, and Brooks SC (1997) Induction of the estrogen specific mitogenic response of MCF-7 cells by selected analogues of estradiol-17 beta: a 3D QSAR study. *J Med Chem* **40**:3659–3669.
- Wold S (1991) Validation of QSARs. *Quant Struct-Act Relat* **10**:191–193.
- Zhu BT, Evaristus EN, Antoniak SK, Sarabia SF, Ricci MJ, and Liehr JG (1996) Metabolic deglucuronidation and demethylation of estrogen conjugates as a source of parent estrogens and catecholesterogen metabolites in Syrian hamster kidney, a target organ of estrogen-induced tumorigenesis. *Toxicol Appl Pharmacol* **136**:186–193.
- Zhu BT and Conney AH (1998) Is 2-methoxyestradiol an endogenous estrogen metabolite that inhibits mammary carcinogenesis? *Cancer Res* **58**:2269–2277.

Address correspondence to: Dr. Alastair Stewart, Department of Pharmacology, University of Melbourne, Victoria 3010, Australia. E-mail: astew@clyde.its.unimelb.edu.au
